

Trading in the Sunshine or in the Shade: Market Impact and Adverse Selection on Hyperliquid

Davide Barone¹ and Fabrizio Lillo¹

¹Scuola Normale Superiore, Pisa, Italy

Abstract

Sunshine trading theory predicts that publicly disclosing trading intentions can reduce adverse selection and attract liquidity provision, lowering execution costs. Evidence is scarce, because explicit preannouncement of large orders is rare in traditional markets. We study Hyperliquid, a fully on-chain limit order book for cryptocurrency perpetual futures, where protocol-native TWAP orders disclose their terms from inception and remain visible while active, a natural form of sunshine trading. Using address-level data, we reconstruct 4.3 million hidden metaorders and compare them with 465,000 visible TWAP executions. The two execution styles differ sharply: hidden metaorders follow front-loaded, U-shaped schedules consistent with transient-impact optimal execution, whereas TWAPs trade nearly uniformly. We test the preannouncement predictions of Admati and Pfleiderer (1991). Visible TWAPs face lower execution costs than comparable hidden metaorders and leave a smaller permanent price impact. Hidden metaorders executed alongside already-visible same-direction TWAP flow incur higher permanent costs: adverse-selection costs shift toward non-announcers. Finally, visible TWAP programs elicit liquidity provision: while active, displayed depth rises and the book tilts toward the absorbing side, the more so the larger the announced order.

1 Introduction

Modeling market impact, i.e., how prices react to orders and trades, is of paramount importance both to understand how information is impounded in prices and to quantify transaction costs. This is even more true and challenging for metaorders, i.e. sequences of orders and trades executed gradually over a long time period and following a single investment decision. Kyle's seminal paper [1] showed that informed traders optimally split large trades over time into child orders in order to balance execution costs against information leakage.

Despite its importance, a satisfactory model and characterization of market impact are still not available for two main reasons: first, metaorder data are rarely available because they are typically proprietary information or must be identified statistically from special labeled data; second, market impact of metaorders in principle depends on many characteristics which might not be observable and/or suitably modeled and therefore the observed properties might be the result of heterogeneous aggregations.

On the empirical side, studies converge toward a series of stylized facts of market impact. The first one is the square-root impact law [2, 3, 4, 5] stating that the expected signed price change, also called temporary impact¹, $I(Q)$ between the beginning and the end of a metaorder of size Q is well described by

$$I(Q) = \pm Y \sigma_D \left(\frac{Q}{V_D} \right)^\delta, \quad (1)$$

where σ_D is daily volatility, V_D daily traded volume, the sign is positive (negative) for buys (sells), and $\delta \simeq 1/2$. More recent analyses show a linear behavior for small volumes or participation

¹This quantity is sometimes also called peak impact. Temporary impact should not be confused with the temporary component of impact, used for example in the Almgren-Chriss model.

rates [6, 7, 8, 9]. Notice that the square-root impact law indicates that the style of trading is not relevant for the price impact, a conclusion that is possibly valid only within some region of the trading trajectories.

Second, a substantial amount of literature [10, 11, 12] investigated the price trajectory during the metaorder execution. It is typically found that the price increases in a concave way as a function of time and, after the end of the metaorder execution, it decays from the peak impact value. The amount of reversion is highly debated, but the evidence unambiguously indicates that market impact has a significant transient component. The long-term limit of the signed price change, named permanent impact of the metaorder, should be related to the information content of the trade. For example, Waelbroeck and Gomes [13] show that after the execution of uninformed metaorders prices tend, on average, to revert toward their pre-execution level.

All these empirical regularities are observed in markets where trades and orders are *anonymous*, i.e. the identity of the investor is not known to the other participants. This element is key to making metaorder execution meaningful: as suggested by Kyle, an informed trader has an incentive to hide her trading intention. In traditional markets, many trading strategies attempt to statistically identify large metaorder executions in order to predict future price changes. It is therefore natural to ask how market impact and price trajectories depend on whether trading intentions are revealed ex ante, i.e. on what the literature terms *sunshine trading*.

Sunshine trading refers to a trading strategy in which large institutional investors pre-announce their intention to trade, for example, disclosing that they will buy or sell a given quantity of an asset over a specified period. The idea, introduced in the market microstructure literature, notably by Admati and Pfleiderer [14], is that transparency can mitigate the classic problem of adverse selection faced by uninformed or liquidity traders. In standard models, large traders who trade secretly are mistaken for informed traders, leading market makers to widen spreads and increase price impact. By contrast, when trades are publicly announced, i.e. “in the sunshine”, other market participants can better infer that the order flow is not information-driven, which reduces uncertainty and can improve execution.

Theoretical predictions are nuanced. On one hand, sunshine trading can lower price impact and trading costs by reducing informational asymmetries and encouraging liquidity provision [14]. On the other hand, public disclosure exposes the trader to front-running or strategic behavior by other market participants, who may trade ahead of the announced order and move prices adversely [15]. As a result, equilibrium models typically predict a trade-off: sunshine trading is more attractive when adverse selection is severe and markets are illiquid, but less desirable when strategic trading and predatory behavior dominate. Overall, the literature highlights that the optimal degree of transparency depends on market structure, the presence of informed traders, and the strategic responses of other agents.

The traditional empirical evidence is relatively narrow because explicit sunshine trading is rare. A relevant quasi-natural experiment is Nasdaq’s “flash orders”, which temporarily revealed marketable orders to a subset of participants before routing. Skjeltorp, Sojli, and Tham [16] find that the introduction of flash functionality improved Nasdaq liquidity and that market quality deteriorated when it was removed, which is broadly consistent with the idea that selective disclosure can mitigate information asymmetry. Related evidence from predictable crude-oil ETF rolls points in the same direction, emphasizing liquidity provision and market resiliency rather than systematic predation [17]. At the same time, both the theoretical and policy literatures stress that transparency is not unambiguously beneficial: if disclosure invites anticipation, predation, or fragmented access to information, it can simply shift price impact earlier rather than eliminate it.

The rise of blockchain-based decentralized exchanges (DEXs) provides a related but distinct setting in which to reconsider sunshine trading. In DeFi, transparency is not only a trader’s disclosure choice, but also a protocol-level design variable that depends on market architecture, block production, and execution ordering. In principle, on-chain data make order flow and

execution outcomes publicly observable and, depending on the protocol design, trading intentions may become visible before execution. This transparency is especially relevant for predatory trading. In traditional markets, the main concern is front-running or strategic order anticipation after disclosure. In DeFi, related mechanisms include front-running, sandwich attacks, transaction-ordering games, and, more generally, MEV extraction [18, 19, 20]. These concerns have motivated several mitigation mechanisms, such as private order flow, private or encrypted mempools, batch auctions, and MEV-protection designs.

This connection with sunshine trading becomes especially close with the development of on-chain central limit order books, which are more directly comparable to classical electronic markets than Automated Market Makers (AMMs). DeFi is therefore a useful laboratory for studying the costs and benefits of transparency.

In this paper, we investigate the role of sunshine trading in price impact and transaction costs by using the unique environment provided by the Hyperliquid blockchain [21]. Hyperliquid is a market for spot and perpetual futures based on a fully on-chain central limit order book (CLOB), i.e., the standard market mechanism in traditional finance. Its architecture makes market activity observable at high frequency: order flow, executions, account-level activity, and the address initiating each action can be reconstructed from public data. More importantly, traders on Hyperliquid can use protocol-native TWAP orders, which automatically split a metaorder into child orders submitted at regular intervals. Since the existence and main parameters of a native TWAP are visible from inception, these orders provide a natural form of *sunshine trading* in a traditional electronic market. Alongside them, we reconstruct *statistical metaorders*, i.e., executions carried out without a protocol-native mechanism and instead implemented through proprietary execution methods. We identify them by aggregating sequences of same-sign market orders from the same address under a standard splitting hypothesis [22, 23, 24]. This allows us to compare automated TWAP programs, whose parent-order parameters are observable from inception, with latent metaorders reconstructed ex post, whose intended size, horizon, and execution rule are not directly observed.

Our main findings are as follows. First, at the aggregate level native TWAPs have systematically lower temporary impact than statistical metaorders, and the two classes differ sharply in execution dynamics: statistical metaorders follow U-shaped execution schedules and markedly non-concave, *double-inflection* price trajectories, with a pronounced peak around completion followed by post-trade decay, consistent with optimal strategic execution under a transient-impact interpretation; native TWAP trajectories, by contrast, are much closer to the smooth, concave square-root path associated with uniform trading in propagator models [12, 7]. We then organize the remaining evidence around the four mechanisms in Admati and Pfleiderer’s analysis of preannouncement. In particular we find that

1. Announcers face lower costs: at the median volatility and conditional on execution characteristics, visible TWAPs have about 9 basis points lower temporary impact than latent metaorders.
2. Announced flow is less informationally adverse: after completion, native TWAPs leave roughly 5 basis points less post-execution price displacement than comparable statistical metaorders.
3. The mirror cost falls on nonannouncers: hidden metaorders executed in the direction of already-visible TWAP flow face higher post-execution price displacement, about 0.8–0.9 basis points for a 10 percentage point increase in same-side visible TWAP dominance.
4. The limit-order book responds to visible execution: during active TWAP windows, displayed depth rises and the book tilts toward the absorbing side; these displayed-liquidity responses scale with announced size and are not explained by favorable pre-trends.

Taken together, the evidence is consistent with a sunshine-trading interpretation, in which publicly visible TWAP flow is on average less informed and its visibility elicits liquidity provision rather than predatory front-running [14, 16].

The rest of the paper is organized as follows. Section 2 describes the Hyperliquid data, the construction of native TWAP and statistical metaorder samples, and the main descriptive statistics. Section 3 studies aggregate market impact, impact trajectories, and execution schedules for the two execution regimes. Section 4 interprets the evidence through the lens of sunshine trading, examining announcer costs, the information content of announced flow, the costs borne by nonannouncers, and the order-book response around visible execution. Section 5 discusses the main limitations of the analysis. Section 6 concludes.

2 A Unique Dataset: Hyperliquid

Our study is based on publicly observable Hyperliquid data. Hyperliquid is a purpose-built Layer-1 blockchain whose state execution is split into two tightly integrated components: *HyperCore*, which hosts fully on-chain spot and perpetual-futures central limit order books (CLOBs), and the *HyperEVM*, a general-purpose smart-contract environment secured by the same consensus [21]. Consensus is implemented via *HyperBFT*, a custom BFT protocol explicitly described as inspired by HotStuff and successors [21, 25]. Importantly, the protocol’s consensus proceeds in *rounds* that may commit an execution block and validator-set parameters evolve over staking epochs [21]. Running nodes is permissionless, while the *active* validator set is selected transparently by stake. As of the documentation accessed on June 1, 2026, the active set is composed of the top 24 validators by delegated stake [21].

Consensus is optimized for end-to-end latency. End-to-end latency is measured as the duration between sending a request and receiving a committed response. For an order placed from a geographically co-located client, end-to-end latency has a median of 0.2 seconds and a 99th percentile of 0.9 seconds [21].

This architecture is especially useful here because executions and account-level activity are observable at transaction frequency and can be reconstructed directly from blockchain data. We obtain the raw historical data through Hydromancer’s Reservoir, a public Hyperliquid data layer [26]. Other recent work also exploits Hyperliquid’s on-chain message data to study market microstructure [27, 28].

We study all 201 Hyperliquid perpetual markets over the period from July 28, 2025, to March 23, 2026. These instruments are crypto perpetual futures: linear contracts written on the oracle index of the corresponding underlying spot asset, with no expiration date and hourly funding. In Hyperliquid’s main contract specification, perpetuals are USDC-margined and USDT-denominated: collateral and traded notionals are accounted for in USDC, while oracle prices are generally denominated in USDT. Accordingly, throughout the paper, order size, market volume, and traded value are measured as USDC notional amounts, which we refer to as USD for familiarity since USDC is pegged one-to-one to the US dollar. The sample contains more than 641 million fills, corresponding to around 365 million market orders and about USD 1.93 trillion in traded volume. Because Hyperliquid trades continuously 24/7, we compute the normalization variables used in the analysis, such as daily traded volume and volatility, over a 24-hour forward-looking window anchored at the metaorder start.

A key feature of the dataset is wallet-level attribution: each action can be assigned to the initiating on-chain address. We identify metaorders in two ways:

- **protocol-native TWAP metaorders:** Hyperliquid offers native TWAP execution as a protocol-level mechanism for splitting a metaorder into a sequence of child orders submitted automatically by validators every 30 seconds. The protocol aims to keep execution close to a time-proportional schedule, subject to a maximum slippage constraint of 3% on each

slice, and allows later slices to increase in size when earlier ones underfill, with catch-up behavior bounded by a maximum of three times the normal suborder size [21]. These native TWAPs are especially relevant for our metaorder and impact analysis because they combine ex-ante observability with ex-post data traceability. On the one hand, the full parent-order instruction becomes publicly visible as soon as the corresponding on-chain transaction is submitted, allowing market participants to observe the existence of the TWAP program and its main characteristics, including direction, total size, execution horizon, and other execution parameters. This makes native TWAPs a protocol-level form of sunshine trading: unlike latent metaorders reconstructed ex post from same-address same-sign trades, they reveal the execution intention before completion.² On the other hand, at the data level, TWAP child executions are identifiable because they are exposed as TWAP slice fills and therefore appear with a *zero transaction hash* (0x00...00); moreover, TWAP-related fills carry a dedicated `twapId` field that groups executions belonging to the same parent TWAP [21].

- **statistical metaorders:** sequences of consecutive same-sign market trades from the same address on the same pair, grouped under a splitting hypothesis when inter-arrival times are below 30 minutes.

After applying our sample restrictions, the final dataset contains approximately 4.3 million statistical metaorders, retaining only reconstructed metaorders with at least 10 child orders, a stricter threshold that reduces false positives from coincidental order clustering, and about 465,000 native TWAP metaorders with at least 5 child orders, as protocol-level identification makes the reconstruction unambiguous even for shorter sequences. We further restrict both samples to executions that complete within 24 hours, consistent with the rolling 24-hour window used to normalize size and volatility, since the traded fraction of a longer execution is not well defined relative to a 24-hour reference window. This cap is immaterial: among reconstructed metaorders with at least 10 child orders it removes only 28,904 orders, 0.7% by count and 1.5% of notional.

For the order-book analysis, we complement the transaction data with a separate sample of limit-order-book snapshots. The downloaded book data cover the investigated markets from December 15, 2025, to March 23, 2026, at one-minute frequency. The raw book files contain 18,701 pair-day panels and about 26.9 million snapshots. For each pair-minute snapshot, we observe the first 20 price levels on both sides of the book, including prices, displayed sizes, and the number of resting orders at each level. The shorter book sample reflects data availability: order-book snapshots are available from December 15, 2025 onward.

2.1 Metaorder Statistics

We begin with descriptive statistics for our sample. We characterize each execution by its order size, physical duration, traded fraction, volume-time duration, participation rate, and number of child orders. For order i , executed on perpetual market m_i , we define notional size, physical duration, and child-order count as

$$Q_i := \sum_{k \in i} p_k |q_k|, \quad T_i := t_{e,i} - t_{s,i}, \quad N_i := \#\{k : k \in i\}.$$

Here q_k is the signed quantity executed in child trade k , p_k is the corresponding execution price, and T_i is measured in minutes. Since the order sign is encoded separately by ϵ_i , Q_i is always positive.

We use two market-volume normalizations. First, we compute the total notional volume traded on the same perpetual market over a rolling 24-hour window starting at the order start

²Active TWAPs can be inspected, for example, on HypurrScan: <https://hypurrscan.io/dashboard>.

time:

$$V_{24h,i} := \sum_{\substack{j: m_j = m_i \\ t_j \in [t_{s,i}, t_{s,i} + 24h)}} p_j |q_j|, \quad \phi_i := \frac{Q_i}{V_{24h,i}}.$$

Thus ϕ_i is the traded fraction. This normalization is not based on calendar days or on a specific time zone: each order is normalized using a trade-specific 24-hour window anchored at its own start time.

Second, we measure the amount of market activity taking place during the execution window of the order:

$$V_i^{\text{exec}} := \sum_{\substack{j: m_j = m_i \\ t_j \in [t_{s,i}, t_{e,i}]}} p_j |q_j|, \quad F_i := \frac{V_i^{\text{exec}}}{V_{24h,i}}, \quad \eta_i := \frac{Q_i}{V_i^{\text{exec}}}.$$

Here F_i is the execution duration measured in volume time, namely the fraction of 24-hour market volume traded during the execution window, while η_i is the average participation rate over the same window. By construction, $\phi_i = \eta_i F_i$. Thus η_i measures how aggressive the order is relative to contemporaneous market activity, rather than relative to daily volume.

Figure 1 reports the distributions of these quantities for the statistical metaorders and native TWAP orders in our sample. The top panels show estimated marginal densities of order notional Q , volume-time duration F , and participation rate η . The bottom-left panel reports the distribution of the number of child orders N , while the remaining bottom panels show the joint distribution of F and η .

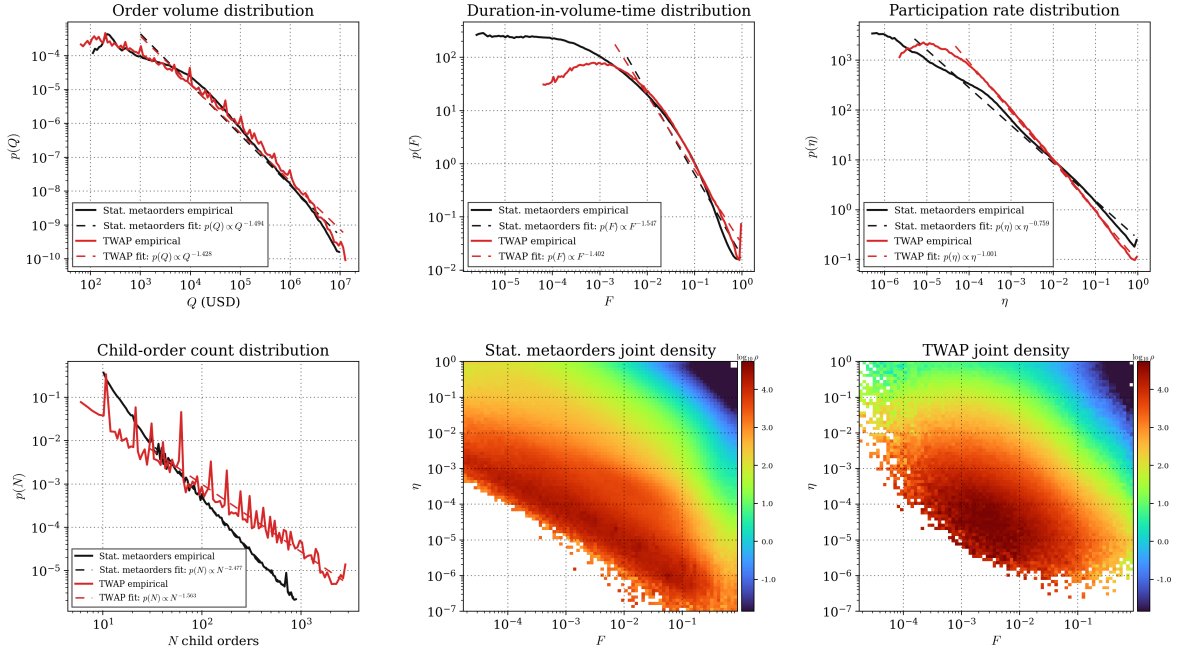


Figure 1: Descriptive statistics for statistical metaorders and native TWAP orders. The top row reports the marginal distributions of order notional Q , volume-time duration $F = V^{\text{exec}}/V_{24h}$, and participation rate $\eta = Q/V^{\text{exec}}$. The bottom-left panel reports the distribution of the number of child orders N . The two remaining bottom panels report log-density heatmaps for the joint distribution of volume-time duration and participation rate, separately for statistical metaorders and native TWAPs. Black lines denote statistical metaorders and red lines denote native TWAPs; dashed lines are tail fits.

The size distributions are broadly comparable in the center but differ in the right tail. The median statistical metaorder has notional about 8.5 thousand USD, while the median

native TWAP is about 9.1 thousand USD. At high quantiles, however, TWAPs are larger: the 95th percentile is roughly 496 thousand USD for TWAPs, compared with 256 thousand USD for statistical metaorders. Thus native TWAPs include a substantial tail of large announced executions.

The volume-time duration distribution shows that TWAPs tend to span slightly more market activity. Median F is about 0.009 for statistical metaorders and 0.012 for native TWAPs, meaning that the median execution takes place over roughly 0.9% and 1.2%, respectively, of the market's rolling 24-hour notional volume. The difference is more pronounced in the upper tail: the 95th percentile of F is about 0.23 for TWAPs, compared with about 0.16 for statistical metaorders. Native TWAPs therefore tend to spread execution over a larger fraction of contemporaneous market volume.

The most important difference is in participation rates. Statistical metaorders are much more aggressive at the median: median η is about 3.4%, while median TWAP participation is about 0.45%. This gap remains large throughout the distribution. The 75th percentile is about 20% for statistical metaorders and about 5.4% for TWAPs. Native TWAPs therefore tend to spread their volume over more market activity, even when their absolute notional is large.

The child-order count distribution shows a further difference in execution style. Statistical metaorders are typically composed of relatively few child orders: the median count is $N = 16$, with a 75th percentile of 25 and a 95th percentile of 73. Native TWAPs have a heavier child-count distribution: their median is $N = 30$, but the 75th and 95th percentiles rise to about 61 and 527, respectively. Thus TWAPs are not only less participatory at a given moment; they also tend to implement that lower participation through a finer slicing of the metaorder.

The joint heatmaps in the bottom row sharpen this picture. In both samples the populated region is organized around a strong downward-sloping envelope in the (F, η) plane. This is the natural geometry of the decomposition $\phi = \eta F$: for a given traded fraction ϕ , orders with larger volume-time duration must have lower participation, while very aggressive orders must be short in volume time. Since extremely large traded fractions are rare in practice, the upper-right region, long in volume time and highly participatory at once, is essentially empty.

Within this common envelope the two populations occupy different regions. Statistical metaorders are more dispersed and place much more mass at high participation rates, especially for short and intermediate values of F . Native TWAPs are shifted toward lower participation and somewhat larger volume-time duration, consistent with scheduled execution that deliberately spreads volume over market activity.

Taken together, the marginal distributions, child-count panel, and joint heatmaps show that the contrast between the two samples is not primarily a difference in order size; it is a difference in execution footprint. Statistical metaorders are typically more concentrated and aggressive, whereas native TWAPs are larger in the right tail, split into more child orders, and executed more passively relative to contemporaneous volume.

3 Market Impact and Price Trajectories

In this section we study market impact at three complementary levels. We first analyze the square-root law, namely the relation between temporary impact and the traded fraction ϕ . This provides an aggregate comparison of execution costs between native TWAPs and statistical metaorders, abstracting from the detailed timing of trades. We then turn to the dynamic dimension of impact, studying both price trajectories during execution and the corresponding execution schedules. These objects allow us to understand how impact builds up over the life of a metaorder and whether different price trajectories are associated with different order-splitting patterns. Finally, we use a simple transient-impact benchmark to interpret the observed shapes.

3.1 Square-Root Law and Impact Surface

We start from the standard aggregate benchmark in the market-impact literature: the dependence of temporary impact on order size expressed as a fraction of 24-hour market volume. For each order, we use the traded fraction $\phi_i = Q_i/V_{24h,i}$, as defined in Section 2.1.

Volatility normalized temporary impact is defined as the signed relative price change between the beginning and the end of execution, rescaled by the daily volatility of the same market:

$$\mathcal{I}_{\text{tmp},i} := \epsilon_i \frac{S_{m_i}(t_{e,i}) - S_{m_i}(t_{s,i})}{S_{m_i}(t_{s,i}) \sigma_{D,i}}, \quad \sigma_{D,i} := \frac{1}{\sqrt{4 \ln 2}} \ln \left(\frac{H_i}{L_i} \right).$$

Here $S_{m_i}(t)$ is the last trade price of market m_i at time t , and $\sigma_{D,i}$ is the daily volatility of the same market. We estimate $\sigma_{D,i}$ over the rolling 24-hour window $[t_{s,i}, t_{s,i} + 24h)$ using the Parkinson estimator [29], where H_i and L_i are the highest and lowest transaction prices observed on market m_i over that window.

We estimate $\mathcal{I}_{\text{tmp}}(\phi)$ by averaging $\mathcal{I}_{\text{tmp},i}$ within bins of ϕ_i . We report our results in Figure 2. The fitted curves are estimated over the range $\phi \geq 10^{-5}$.

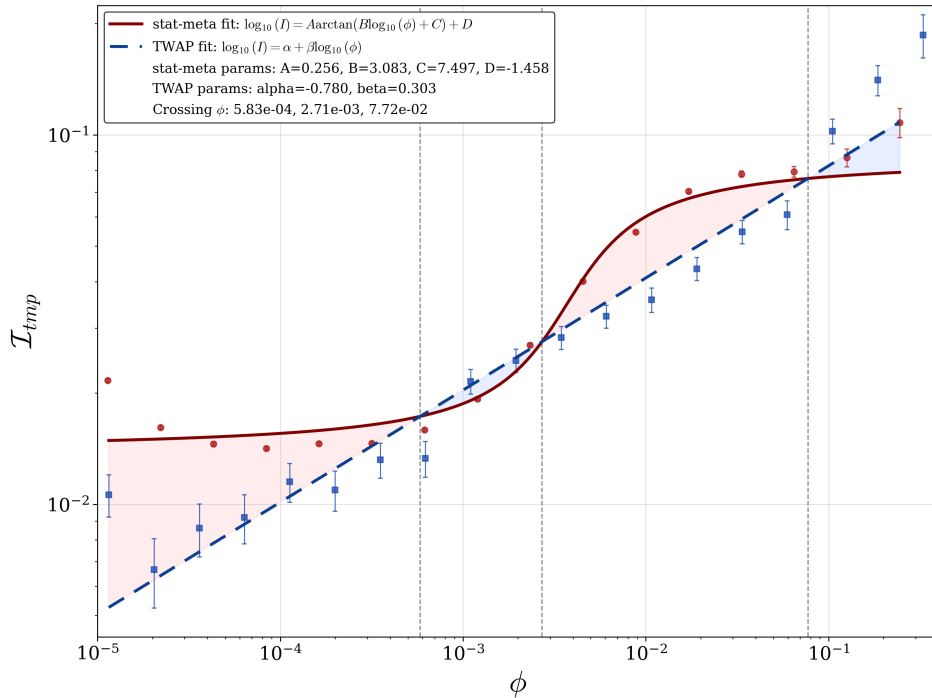


Figure 2: Temporary market impact \mathcal{I}_{tmp} as a function of the 24-hour traded fraction $\phi = Q/V_{24h}$ for statistical metaorders and native TWAP orders. Points denote binned means and error bars denote ± 1 standard error. The plot is shown on double-logarithmic axes. The solid red curve is the fitted statistical-metaorder relation $\log_{10}(\mathcal{I}_{\text{tmp}}) = A \arctan(B \log_{10}(\phi) + C) + D$, while the dashed blue curve is the fitted TWAP power law $\log_{10}(\mathcal{I}_{\text{tmp}}) = \alpha + \beta \log_{10}(\phi)$. Vertical dashed lines mark the intersections of the two fitted curves.

The two populations are not described by a common aggregate impact curve. Native TWAP orders display an approximately linear relation in log-log scale over the displayed range:

$$\log_{10} \mathcal{I}_{\text{tmp}}^{\text{TWAP}}(\phi) = \alpha + \beta \log_{10} \phi,$$

with estimates $\hat{\alpha} = -0.780 \pm 0.004$ and $\hat{\beta} = 0.303 \pm 0.002$. Equivalently, $\mathcal{I}_{\text{tmp}}^{\text{TWAP}}(\phi) \propto \phi^{0.303}$, with an exponent well below the square-root benchmark.

Statistical metaorders display a markedly different shape. Their binned impact is fitted by the nonlinear arctangent specification

$$\log_{10} \mathcal{I}_{\text{tmp}}^{\text{stat}}(\phi) = A \arctan(B \log_{10} \phi + C) + D,$$

with estimates

$$\hat{A} = 0.256 \pm 0.003, \quad \hat{B} = 3.083 \pm 0.081, \quad \hat{C} = 7.497 \pm 0.204, \quad \hat{D} = -1.458 \pm 0.002,$$

and $R^2 = 0.968$ across the fitted bins. This functional form captures the flattening of statistical-metaorder impact at low traded fractions, the sharp increase over intermediate traded fractions, and the subsequent saturation at high ϕ .

The fitted curves intersect at approximately

$$\phi = 5.83 \times 10^{-4}, \quad \phi = 2.71 \times 10^{-3}, \quad \phi = 7.72 \times 10^{-2}.$$

Thus the ordering of statistical-metaorder and TWAP impact is not constant over the support. The main point is not the precise location of these crossings, but the fact that the two samples have different aggregate shapes: TWAP impact is close to a regular power law, whereas statistical metaorder impact is strongly curved and saturating. In this sample, therefore, a single square-root law does not provide a universal description of temporary impact.

The traded fraction ϕ summarizes order size in a single variable, but it does not distinguish between two economically different dimensions: how long the order is executed and how aggressively it participates in the market. To separate these effects, we use the decomposition

$$\phi_i = \eta_i F_i,$$

where F_i is volume-time duration and η_i is the average participation rate, both defined in Section 2.1.

Pooling statistical metaorders and native TWAPs, we estimate the temporary-impact surface in $(\log_{10} \eta, \log_{10} F, \log_{10} \mathcal{I}_{\text{tmp}})$ by binning orders in the (η, F) plane and computing the average temporary impact in each populated bin. We then fit a separable power law to the resulting pooled binned surface:

$$\mathcal{I}_{\text{tmp}}(\eta, F) = Y \eta^\delta F^{\gamma_1}.$$

This specification provides a good description of the aggregated surface, with

$$\hat{Y} = 0.186 \pm 0.004, \quad \hat{\delta} = 0.118 \pm 0.003, \quad \hat{\gamma}_1 = 0.306 \pm 0.003,$$

and $R^2 = 0.886$.

Overall, the fitted pooled surface varies more along the duration dimension than along the participation-rate dimension. The exponent on F is about 0.31, whereas the exponent on η is about 0.12. Thus, conditional on the decomposition $\phi = \eta F$, the amount of market activity spanned by the execution is the stronger predictor of temporary impact. Participation still enters positively, but with a substantially smaller elasticity. The one-dimensional square-root-law benchmark is therefore incomplete: orders with the same traded fraction can have different impact depending on how that fraction is split between participation rate and volume-time duration. This contrasts with Zarinelli et al. [6], who find a joint power-law fit with both exponents close to one half. In our pooled Hyperliquid sample, both elasticities are smaller and the surface is much more tilted toward volume-time duration. Thus, the deviation from the square-root benchmark is not a balanced dependence on η and F , but mainly reflects the dominance of the duration channel.

3.2 Impact Trajectories and Execution Schedules

The previous analysis compresses each metaorder into a single temporary-impact measure. This is useful for comparing aggregate execution costs, but it discards the dynamic information contained in the price path during execution. We therefore study impact trajectories to compare how impact builds up over the life of a metaorder and how it evolves after completion.

For this analysis, time is measured in physical time. For each metaorder i , let $T_i := t_{e,i} - t_{s,i}$ be its clock-time duration. If t denotes elapsed time from the start of the metaorder, normalized physical time is $\tau := t/T_i$, so that $\tau = 0$ corresponds to the start of execution and $\tau = 1$ to completion. Values $\tau < 0$ and $\tau > 1$ describe the pre- and post-execution windows shown in the figure. For each order i , we construct the signed impact trajectory

$$\mathcal{I}_i(\tau) = \frac{\epsilon_i}{\sigma_{D,i}} \left(\frac{S_i(\tau)}{S_i(0)} - 1 \right),$$

where $S_i(\tau) := S_{m_i}(t_{s,i} + \tau T_i)$ denotes the last trade price of market m_i at normalized physical time τ .

To compare trajectory shapes across orders with different aggregate impact scales, we normalize each signed trajectory by the fitted temporary impact predicted for its execution class. Let $g(i) \in \{\text{stat}, \text{TWAP}\}$ denote the class of order i . We define

$$\tilde{I}_i(\tau) = \frac{\mathcal{I}_i(\tau)}{\hat{\mathcal{I}}_{\text{tmp}}^{g(i)}(\phi_i)},$$

where

$$\log_{10} \hat{\mathcal{I}}_{\text{tmp}}^{\text{stat}}(\phi) = A \arctan(B \log_{10} \phi + C) + D, \quad \log_{10} \hat{\mathcal{I}}_{\text{tmp}}^{\text{TWAP}}(\phi) = \alpha + \beta \log_{10} \phi.$$

are the fitted aggregate-impact laws with the estimated parameters. This normalization removes, separately for the two execution mechanisms, the average dependence of temporary impact on traded fraction and makes the figure mainly informative about trajectory shape rather than absolute impact levels. It does not, however, force the trajectory to equal one at completion: the denominator is the impact *predicted* by the aggregate law at ϕ_i , not the realized completion impact $I_i(1)$; each panel averages order-level ratios, which need not coincide with the ratio of averages; and the law is pooled in ϕ while the panels condition on (T, η) . The completion level $\tilde{I}_i(1)$ is therefore itself informative, measuring how far realized impact in each (T, η) cell departs from the one-dimensional square-root law.

Figure 3 compares average impact trajectories after conditioning jointly on clock-time duration T_i and participation rate η_i . On the normalized left axis, native TWAP trajectories rise in a concave, strictly increasing way over the execution interval; in several panels, however, they lie substantially below one, that is, below the impact predicted by the aggregate square-root law. Plotted in signed basis points on the right vertical axis, the same trajectories display the typical concave, square-root-like profile documented in the empirical literature, rising as execution proceeds and well fitted by a power law of the form $A\tau^\gamma$ [12, 6].

Statistical metaorders display a different dynamic pattern. Their trajectories are markedly non-concave, with a double-inflection shape, a sharp peak around completion, and a more pronounced post-trade decay. This pattern is not an artifact of the normalization: the same qualitative shape is also observed when trajectories are expressed in signed basis points. This suggests that the difference between statistical metaorders and native TWAPs is not only a difference in impact levels, but also in the way impact accumulates during execution and relaxes afterwards. Such patterns are consistent with optimal execution under transient-impact models [30, 31], which prescribes a U-shape in the trading velocity.

The pre-execution segments in Figure 3 reveal a further difference between the two regimes: the price conditions under which execution begins. Statistical metaorders start on average against

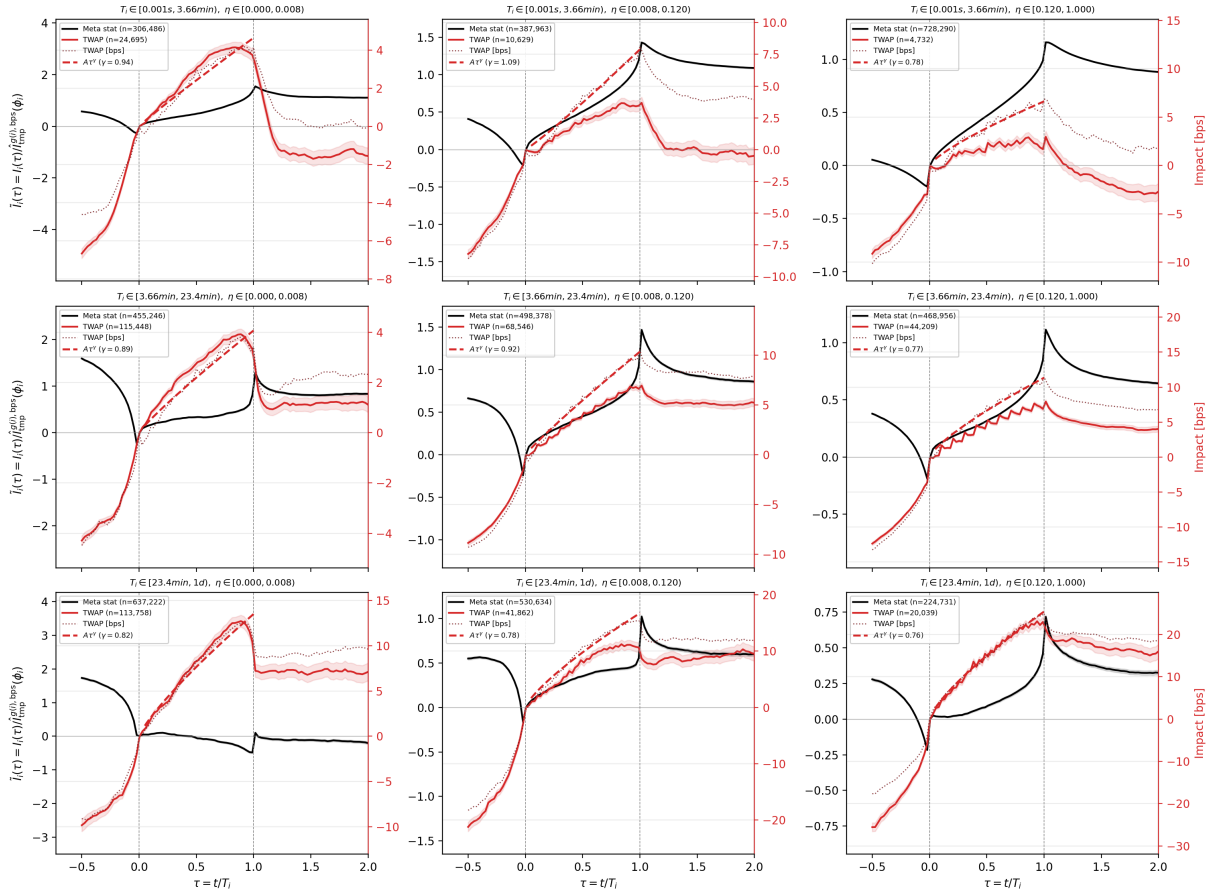


Figure 3: Average signed impact trajectories for statistical metaorders and native TWAP orders, conditional on clock-time duration T_i and participation rate η_i . The nine panels correspond to a 3×3 sort: rows by T_i and columns by η_i , both ordered increasingly from left to right and from top to bottom. The horizontal axis reports normalized physical time $\tau = t/T_i$, where t is elapsed time from the start of the metaorder; $\tau = 0$ marks the start of execution and $\tau = 1$ marks completion. Each panel uses two independent vertical axes: the *left axis* reports the impact-law-normalized trajectory $\tilde{I}_i(\tau) = \mathcal{I}_i(\tau)/\hat{\mathcal{I}}_{\text{tmp}}^{g(i)}(\phi_i)$, while the *right axis* reports the corresponding native TWAP trajectory in signed basis points. Black solid lines denote statistical metaorders and red solid lines native TWAPs on the left axis; shaded bands denote ± 1 SEM around the mean trajectory. The dotted dark-red line shows the TWAP trajectory in basis points on the right axis, and the dashed red line reports a power-law fit $A\tau^\gamma$.

the recent price movement: over a 30-minute window before the start, the signed pre-start return is -7.0 basis points on average (median -3.9), and only 47.7% of pre-start moves are in the direction of the subsequent order. Native TWAPs begin with the trend: $+18.2$ basis points on average (median $+13.5$), with a same-direction share of 58.4%. This is a property of the entry decision rather than of the market states the two groups select: measured 24 hours before the start, the gap vanishes (-0.2 basis points, $p = 0.73$). Latent metaorders are thus on average contrarian, while announced TWAPs are trend-following.

To understand whether these differences in price trajectories are related to differences in trading schedules, we next study the cumulative fraction executed over normalized physical time. Let $Q_i(\tau)$ denote the amount executed by elapsed time τT_i , with $\tau \in [0, 1]$. We define the execution schedule as

$$C_i(\tau) := \frac{Q_i(\tau)}{Q_i}.$$

Thus $C_i(\tau)$ is the cumulative fraction of the metaorder executed by normalized physical time τ . A linear schedule, $C_i(\tau) = \tau$, corresponds to uniform execution in physical time.

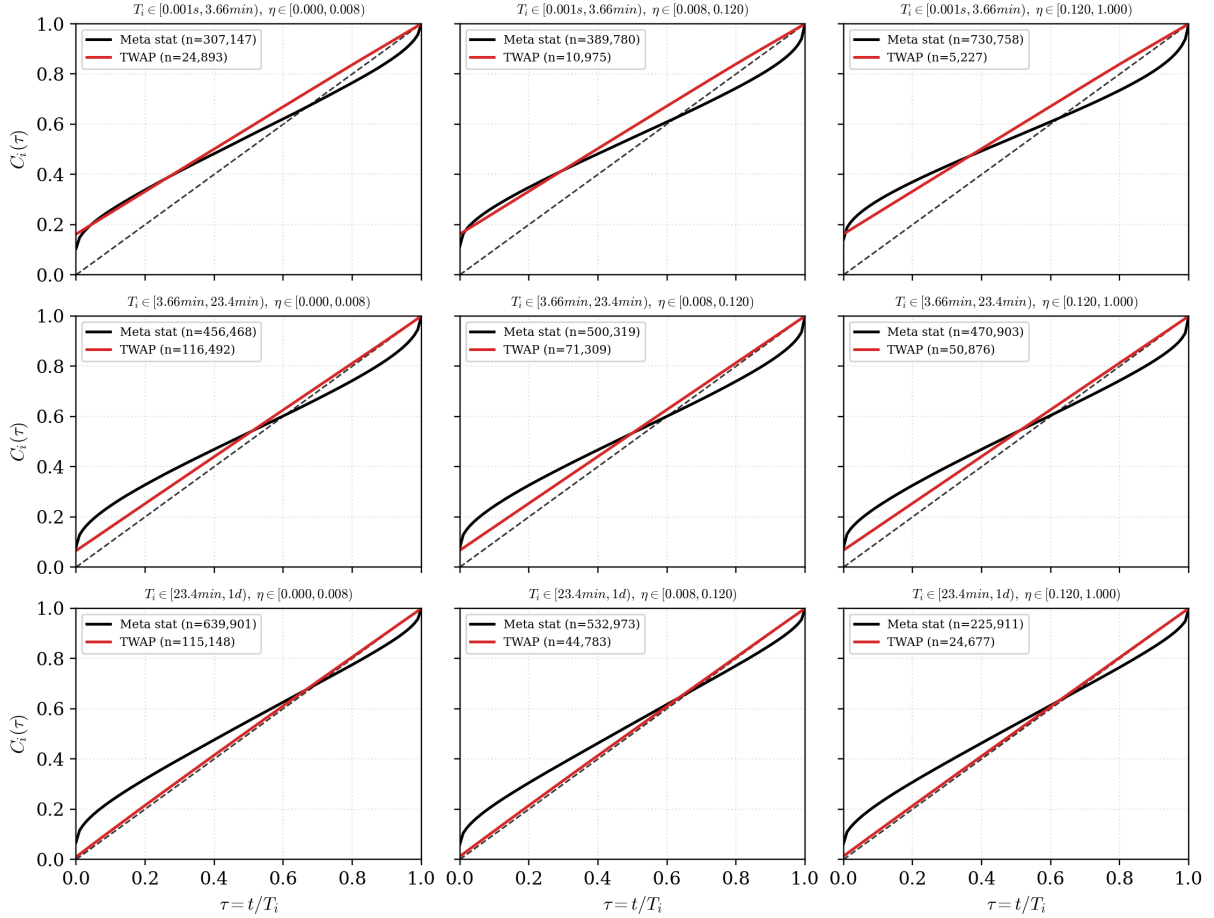


Figure 4: Average normalized execution schedules for statistical metaorders and native TWAP orders, conditional on clock-time duration T_i and participation rate η_i . The horizontal axis reports normalized physical time $\tau = t/T_i \in [0, 1]$, and the vertical axis reports the execution schedule $C_i(\tau)$. Black lines denote statistical metaorders and red lines native TWAP orders; the dashed diagonal is the linear benchmark corresponding to uniform execution in physical time.

Figure 4 shows that the difference in trajectories is mirrored by a difference in execution schedules. Native TWAP orders are, by construction, a linear benchmark: on Hyperliquid, the metaorder is split into regularly spaced child orders over the execution interval. The positive intercept visible in the figure is mechanical, since the first child trade is assigned to $\tau = 0$ in our measurement of the cumulative schedule. Statistical metaorders, instead, are systematically non-linear: the execution rate is about 1.5–1.7 times the uniform benchmark over the first decile of normalized time, falls to 0.6–0.8 in the middle of the window, and rises again to 1.1–1.4 over the last decile, before a final step at $\tau = 1$ that contains the mechanical mass of the last child order ($\approx 1/N$, analogous to the intercept at $\tau = 0$). This asymmetric, front-loaded U-shape is typical of optimal execution under a transient-impact model with risk aversion.

A natural concern is that the endpoint of a reconstructed metaorder is defined ex post by its last trade, so a trader who stops *because* the price has moved would mechanically concentrate peak impact at completion. The schedules argue against this reading. Price-contingent stopping at a constant trading rate would leave the interior schedule flat, with only a final mechanical step of size $\approx 1/N$; instead, the acceleration builds over the entire last decile. Moreover, the shape does not respond to the realized price path: splitting metaorders by the sign of the in-window price move, both groups show the same terminal acceleration (1.01 vs. 1.03 times the uniform

benchmark). Completion is anticipated by the execution program, not triggered by the price.

Taken together, Figures 3 and 4 support a transient-impact interpretation. Nearly uniform TWAP execution generates smooth, square-root-like trajectories, whereas the U-shaped schedules of statistical metaorders are associated with stronger curvature, completion peaks, and S-shaped trajectories. We do not claim structural identification of an optimal-execution model; the evidence is more modest, but it is consistent with the transient-impact model. Appendix A reviews the price trajectories expected under the transient impact model and their relation with the empirical data.

4 Sunshine Trading

The term *sunshine trading* refers to the preannouncement of a trader’s intended order before execution. Admati and Pfleiderer [14] analyze this mechanism by separating two effects of preannouncement. The first is an informational effect. In their baseline model with heterogeneous private information and zero entry costs, all speculators are already present in the market. Preannouncement therefore does not change the size of the market; instead, it changes what the market learns from order flow. If the announced demand is known to come from liquidity traders it is separated from the order flow that may be privately informed. In this case, preannouncement lowers the expected trading costs of announcers, raises the expected trading costs of nonannouncers, lowers the aggregate expected trading costs of liquidity traders, and makes prices more informative.

The second effect operates through the participation of liquidity suppliers. In a separate model with no private information but positive entry costs, speculators must pay a fixed cost to enter the risky-asset market. Without preannouncement, entry is based on the distribution of liquidity demand. With preannouncement, entry can instead condition on the realized announced demand. When entry costs are sufficiently high, this can increase the effective supply of liquidity around announced orders and reduce announcers’ expected trading costs. When entry costs are low, however, most speculators would enter even without preannouncement, so the benefit from coordinating entry is limited and the effect on trading costs can reverse. Thus, the model predicts a clear informational selection effect, while the liquidity-supply channel depends on the importance of the entry margin.

Hyperliquid provides an empirical analogue of these mechanisms. Protocol-native TWAP orders are visible while active and reveal the main features of the execution program before completion. Statistical metaorders, by contrast, are inferred only ex post from same-address same-sign trading sequences. The relevant comparison is therefore not simply between two execution algorithms, but between two execution regimes that differ in ex-ante observability. Native TWAPs play the role of visible liquidity demand, while statistical metaorders provide a benchmark for latent order splitting.

We organize the evidence around four empirical counterparts of the Admati–Pfleiderer results. First, we test whether visible TWAPs have lower execution costs than otherwise comparable hidden metaorders, as predicted for announcers in the informational model and in the costly-entry model when the entry margin is sufficiently important. Second, we test whether visible TWAP flow is less informationally adverse by studying post-execution price persistence: if announced flow is less informed, it should leave a smaller permanent price displacement after completion. Third, we ask whether visible TWAP activity worsens the execution costs of hidden non-announcing traders, as in the adverse-selection effect on nonannouncers, or instead benefits them through a liquidity-supply externality. Fourth, we study the limit-order-book response around active TWAP windows as the observable counterpart of the market’s liquidity-supply response to preannounced execution.

Since traders self-select into native TWAP execution, the comparison should be interpreted as an equilibrium comparison between visible and latent execution regimes, rather than as a

randomized treatment of order visibility.

4.1 Trading Costs of Announcers

The first empirical prediction concerns the trading costs of announcing traders. If preannouncement separates visible liquidity demand from potentially informed order flow, or if it attracts additional liquidity supply when entry margins are important, announced orders should face lower execution costs than comparable latent orders.

We test this prediction by comparing the volatility-normalized temporary impact $\mathcal{I}_{\text{tmp},i}$ of protocol-native TWAPs and statistical metaorders. We compare groups on the common support of (η_i, F_i) , where $\phi_i = \eta_i F_i$, to account for the distributional differences between the two samples documented in subsection 2.1. We also restrict the analysis to the second and third participation columns of the 3×3 duration–participation sort, excluding the lowest-participation region where signed price changes are dominated by idiosyncratic volatility rather than execution impact. We further require $F \in [3 \times 10^{-4}, 1]$ and at least 50 observations per group in each (η, F) cell.

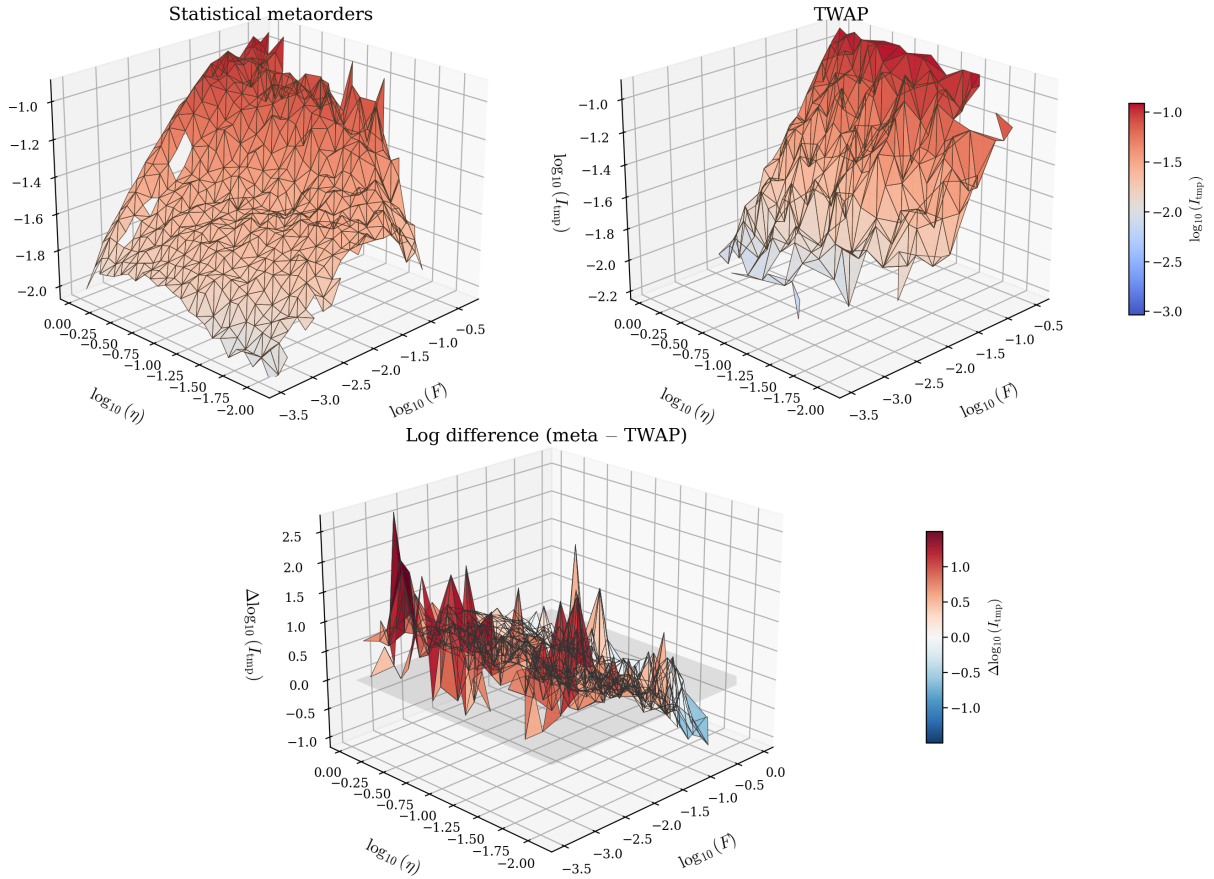


Figure 5: Common-support temporary-impact surfaces for statistical metaorders and native TWAPs. The top-left panel reports the surface for statistical metaorders, the top-right panel the surface for native TWAPs, and the bottom panel the log difference $\log_{10}(\mathcal{I}_{\text{tmp}}^{\text{stat}}/\mathcal{I}_{\text{tmp}}^{\text{TWAP}})$. The plotted grid contains 562 populated common-support cells, representing 2,543,655 statistical metaorders and 200,916 native TWAPs. The log-difference panel is computed on the 470 cells in which both groups have positive mean temporary impact. Positive values in the bottom panel indicate cells in which statistical metaorders have larger volatility-normalized temporary impact than native TWAPs.

Figure 5 reports the resulting surfaces. Statistical metaorders have larger temporary impact than native TWAPs in 81% of the populated common-support cells. Restricting to the cells

where both means are positive, this fraction is 79%, and weighting cells by the smaller of the two group counts raises it to 88%. The median log difference is 0.37, corresponding to a median impact ratio of about 2.3.

The gap is concentrated at short and intermediate volume-time durations. For $F < 3 \times 10^{-3}$, statistical metaorders exceed native TWAPs in every positive cell, with a median ratio of about 5.4. For $3 \times 10^{-3} \leq F < 3 \times 10^{-2}$, the median ratio is about 3.1. For $F \geq 3 \times 10^{-2}$, the two surfaces nearly coincide, with a median ratio close to one and an unstable sign. Thus, conditional on similar participation and volume-time duration, latent statistical metaorders generate larger temporary price impact than visible TWAPs over most of the economically relevant common support.

To summarize the comparison parametrically, we fit the separable power-law specification

$$\mathcal{I}_{\text{tmp}}^g(\eta, F) = Y_g \eta^{\delta_g} F^{\gamma_g}, \quad g \in \{\text{stat}, \text{TWAP}\}. \quad (2)$$

For statistical metaorders, the fitted parameters are $Y_{\text{stat}} = 0.202 \pm 0.006$, $\delta_{\text{stat}} = 0.150 \pm 0.006$, and $\gamma_{\text{stat}} = 0.303 \pm 0.005$, with $R^2 = 0.889$. For native TWAPs, the corresponding estimates are $Y_{\text{TWAP}} = 0.294 \pm 0.013$, $\delta_{\text{TWAP}} = 0.010 \pm 0.011$, and $\gamma_{\text{TWAP}} = 0.622 \pm 0.011$, with $R^2 = 0.868$.

The fitted elasticities show that the two surfaces differ in shape, not only in level. For native TWAPs, the participation exponent is consistent with zero: conditional on volume-time duration, participation contains little additional information about temporary impact. For statistical metaorders, participation has a small but significant elasticity, while the duration elasticity is lower. As a result, the two surfaces cross: statistical metaorders dominate at short volume-time durations, and the gap narrows as F increases.

As an order-level check of the surface evidence, we estimate a pooled interaction regression on the same common-support sample. We use median-centered log covariates, so that the TWAP indicator is evaluated at the median execution profile. Specifically, for $x \in \{Q, F, \eta, \sigma\}$, let $x_i^c = \log x_i - \text{med}_{j \in \mathcal{S}}(\log x_j)$, where \mathcal{S} denotes the common-support estimation sample. We estimate

$$\begin{aligned} \mathcal{I}_{\text{tmp},i} = & \alpha + \theta D_i^{\text{TWAP}} + \beta_Q Q_i^c + \beta_F F_i^c + \beta_\eta \eta_i^c + \beta_\sigma \sigma_i^c \\ & + D_i^{\text{TWAP}} (\kappa_Q Q_i^c + \kappa_F F_i^c + \kappa_\eta \eta_i^c + \kappa_\sigma \sigma_i^c) + \mu_{m(i)} + \lambda_{h(i)} + \delta_{d(i)} + u_i. \end{aligned} \quad (3)$$

Here D_i^{TWAP} is an indicator equal to one for native TWAPs, $\mu_{m(i)}$ are market fixed effects, $\lambda_{h(i)}$ are start-hour fixed effects, and $\delta_{d(i)}$ are start-day fixed effects. Standard errors are clustered by start day. The coefficients β_x describe how temporary impact varies with order size, duration, participation, and volatility for statistical metaorders, while $\beta_x + \kappa_x$ gives the corresponding slope for native TWAPs. The coefficient θ measures the TWAP–statistical gap at the median execution profile, within the same market, start hour, and start day.

The estimated TWAP gap is $\hat{\theta} = -0.0177$, with standard error 0.0010. At the pooled median volatility, $\sigma \simeq 0.050$, this corresponds to about 8.9 basis points lower temporary impact for a native TWAP relative to a statistical metaorder with the same reference execution profile. Thus, the order-level regression confirms the main message of the surface comparison: the lower cost of visible execution is not only due to TWAPs occupying a different region of the (η, F) plane.

Because the two regimes enter under opposite price conditions (Section 3.2), part of the gap could in principle reflect the continuation or reversal of pre-existing trends rather than execution costs. Adding the signed pre-start return as a control leaves the estimate essentially unchanged, at $\hat{\theta} = -0.0173$, about 8.7 basis points at the median volatility: the announcer discount is not an artifact of entry conditions.

Table 1 shows that the two regimes differ not only in average impact, but also in the margins along which impact varies. For statistical metaorders, temporary impact increases significantly with notional size, volume-time duration, and participation. For native TWAPs, impact also increases with notional size and volume-time duration, but the participation slope is small and

Regressor	Statistical metaorders	Native TWAPs
$\log Q$	0.00829*** (0.00042)	0.00650*** (0.00048)
$\log F$	0.00419*** (0.00061)	0.00690*** (0.00085)
$\log \eta$	0.00342*** (0.00048)	-0.00058 (0.00071)
$\log \sigma$	-0.01485*** (0.00113)	0.00109 (0.00123)

Table 1: Order-level regression slopes for volatility-normalized temporary impact on the common support of Figure 5. The first column reports β_x , the slope for statistical metaorders; the second reports $\beta_x + \kappa_x$, the corresponding slope for native TWAPs. Standard errors, clustered by start day, are in parentheses. Significance levels: * $p < 0.10$, ** $p < 0.05$, *** $p < 0.01$.

statistically indistinguishable from zero. Thus, conditional on the amount of market activity spanned by the order, participation remains an important cost margin for latent metaorders but not for visible TWAPs. This reinforces the interpretation from the fitted surfaces: statistical metaorders are penalized when they execute aggressively relative to contemporaneous volume, whereas TWAP costs are driven mainly by size and exposure over volume time.

Overall, the evidence is consistent with the announcer-cost prediction of sunshine trading. Visible TWAPs have lower temporary impact than latent statistical metaorders over most of the common support, especially for executions that are concentrated in (volume) time. The parametric fit reinforces this result: the two regimes are not related by a simple level shift, but by different elasticities to participation and volume-time duration. In this sense, the transparent execution channel is associated with lower trading costs for announcers, while the crossing of the surfaces suggests that the benefit of visibility is strongest for relatively concentrated executions.

4.2 Information Content of Announced Flow

The second implication concerns the information content of announced order flow. In the informational model, preannouncement identifies part of liquidity demand as uninformed, making equilibrium prices more informative. In our setting, however, traders choose whether to use native TWAP execution, so the uninformed nature of announced flow is not imposed by the protocol. The empirical question is whether visible TWAP flow is less informationally adverse than latent statistical metaorders.

We use post-execution price dynamics as a reduced-form measure of informational content. Temporary impact at completion can reflect two components. One is transitory liquidity pressure generated by the execution itself, which should partly revert once the order is completed. The other is information incorporated into prices, which should be more permanent. Thus, if native TWAPs are less informationally adverse than statistical metaorders, their impact should decay more quickly after completion and leave a smaller permanent price displacement.

Figure 6 reports post-execution impact decay after normalizing each trajectory by its value at completion. This normalization sets all trajectories equal to one at $\tau = 1$, so that the comparison focuses on the fraction of completion impact that remains after execution. In most bins, statistical metaorders retain a larger fraction of their completion impact over the post-trade window, while native TWAP orders relax more quickly. The main exceptions are concentrated in longer-duration bins, where normalized TWAP paths remain closer to the statistical-metaorder paths or decay more slowly. Overall, this pattern suggests that the impact of visible TWAP flow is more transitory, while a larger component of the impact of statistical metaorders remains incorporated into prices.

We quantify this difference using permanent impact. For $\tau \in \{1.5, 2, 3, 4\}$, we evaluate the price $S_i(\tau)$, defined in Section 3.2, at post-execution horizons expressed in multiples of the

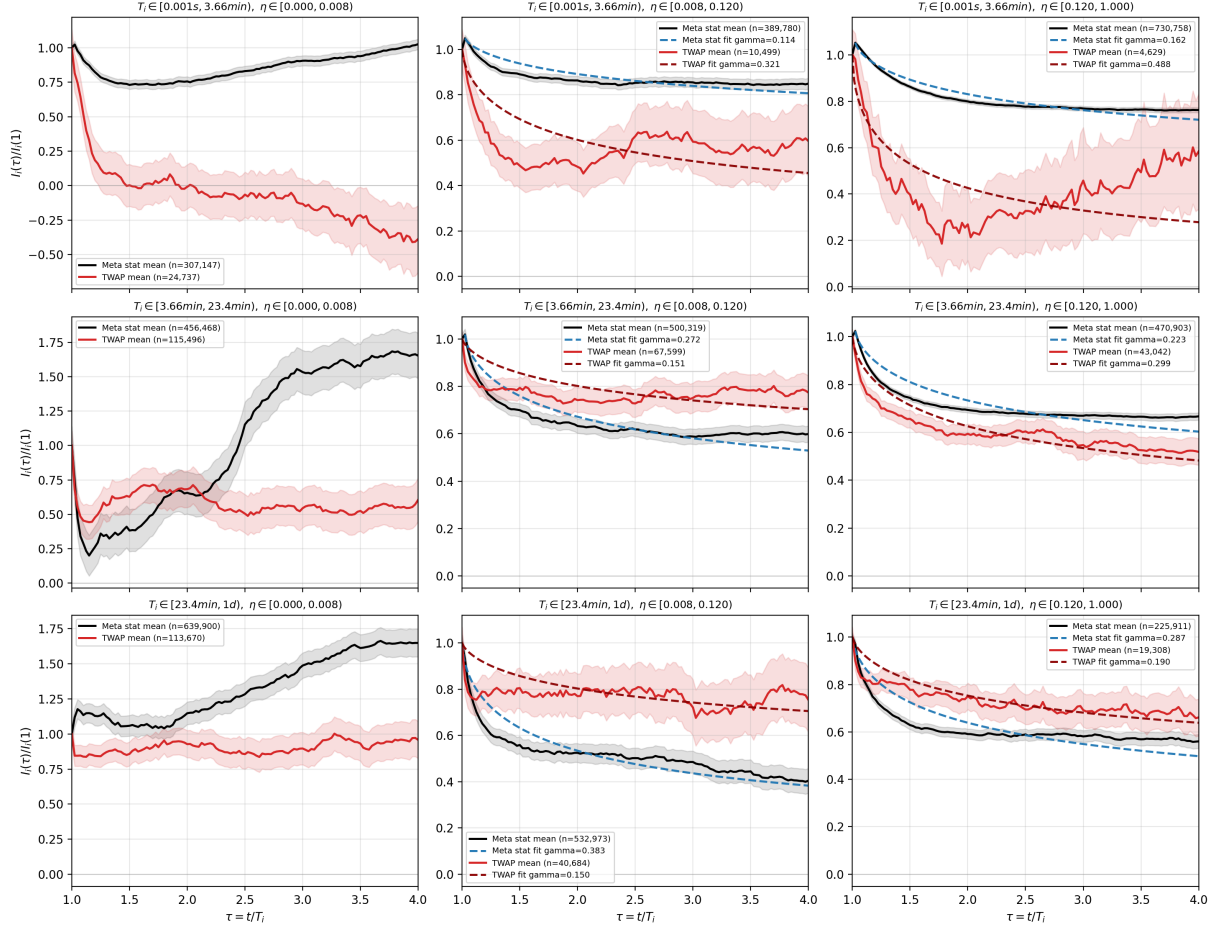


Figure 6: Post-execution decay of signed impact across duration–participation bins, with each trajectory normalized by its value at completion. The horizontal axis reports normalized physical time $\tau = t/T_i$, where $\tau = 1$ marks the end of execution and the plotted interval after $\tau = 1$ corresponds to the post-trade window. Black solid lines denote statistical metaorders and red solid lines native TWAP orders; shaded bands denote ± 1 standard error. Blue and dark-red dashed lines are power-law fits to post-execution decay, estimated separately for statistical metaorders and TWAPs.

order’s own duration. We define

$$I_i^{\text{perm}}(\tau) = 10^4 \epsilon_i \frac{S_i(\tau) - S_i(0)}{S_i(0)}. \quad (4)$$

This object measures the signed price displacement from the beginning of the metaorder to a post-execution horizon, which we refer to as the permanent price impact of the metaorder.

For each horizon τ , we estimate

$$I_i^{\text{perm}}(\tau) = \alpha + \beta_{\text{TWAP}} D_i^{\text{TWAP}} + \gamma_1 \sqrt{\phi_i} + \gamma_2 \eta_i + \gamma_3 \log T_i + \gamma_4 \sigma_{D,i} + \mu_{\text{coin}(i)} + \mu_{\text{hour}(i)} + \mu_{\text{day}(i)} + u_i. \quad (5)$$

We also estimate a specification that excludes the traded-fraction control,

$$I_i^{\text{perm}}(\tau) = \alpha + \beta_{\text{TWAP}} D_i^{\text{TWAP}} + \gamma_1 \eta_i + \gamma_2 \log T_i + \gamma_3 \sigma_{D,i} + \mu_{\text{coin}(i)} + \mu_{\text{hour}(i)} + \mu_{\text{day}(i)} + u_i. \quad (6)$$

The fixed effects are for asset, start hour, and start day, and standard errors are clustered by calendar day. The coefficient of interest is β_{TWAP} : a negative value means that, conditional on the included controls and fixed effects, native TWAPs leave a smaller permanent price

Spec.	$\tau = 1.5$	$\tau = 2$	$\tau = 3$	$\tau = 4$
Eq. (5)	-5.41*** (0.69)	-4.99*** (0.70)	-5.45*** (0.84)	-5.23*** (0.93)
Eq. (6)	-3.60*** (0.64)	-3.25*** (0.67)	-3.79*** (0.81)	-3.66*** (0.91)

Table 2: TWAP discount in permanent impact. The table reports the coefficient β_{TWAP} on D_i^{TWAP} from Eqs. (5)–(6). The dependent variable is $I_i^{\text{perm}}(\tau)$, measured in basis points. Standard errors, clustered by calendar day, are in parentheses. All specifications include asset, start-hour, and start-day fixed effects. The sample contains approximately 3.09 million observations and 239 day clusters. *** $p < 0.001$.

displacement than statistical metaorders.

Table 2 shows that native TWAPs leave a smaller permanent price displacement than statistical metaorders at every post-execution horizon. In the baseline specification, the TWAP coefficient is between -5.0 and -5.5 basis points and highly significant across all horizons.

The specification without the traded-fraction control gives the same qualitative result, with coefficients of about -3.3 – -3.8 basis points. The attenuation indicates that part of the gap is related to differences in relative size, but the TWAP discount does not depend on controlling for ϕ_i .

Entry conditions are a sharper concern for permanent impact: since statistical metaorders are on average contrarian, part of their larger permanent footprint could reflect the reversal of the pre-entry price dip rather than information. Controlling for the signed pre-start return attenuates the TWAP coefficient by 5–11% across horizons (from -5.4 to -5.1 basis points at $\tau = 1.5$, and from -5.2 to -4.7 at $\tau = 4$), leaving the conclusion unchanged.

Taken together, the decay curves and the finite-horizon regressions point to the same conclusion. Native TWAPs do not only generate lower temporary impact at completion; they also leave a smaller permanent price displacement. This is consistent with the informational channel in Admati–Pfleiderer: the price displacement that survives execution is the component most plausibly tied to information, and it is systematically smaller for the visible execution channel.

4.3 Trading Costs of Nonannouncers

The third test shifts the focus from traders who choose visible execution to hidden traders who execute while visible TWAP flow is active. The key question is whether the presence of announced order flow changes the cost of latent metaorders. If visible TWAPs are interpreted by the market as relatively uninformed liquidity demand, then hidden same-side trading may become a more adversely selected residual category and therefore face higher execution costs. At the same time, visible TWAP activity may also attract liquidity supply, in which case hidden traders could benefit rather than suffer. We therefore test whether statistical metaorders become more or less costly when they overlap with native TWAP flow.

The direction of the overlapping TWAP flow is central for this test. A same-side TWAP is visible order flow in the same direction as the focal statistical metaorder. If visible same-side flow is perceived as less informationally adverse, then the remaining hidden flow in that direction should be priced as more adversely selected. This is the direct analogue of the Admati–Pfleiderer prediction for nonannouncers. By contrast, opposite-side TWAP flow has a different mechanical interpretation: it pushes against the focal order direction and can reduce the focal’s signed cost. We therefore decompose contemporaneous TWAP dominance by side.

For each focal statistical metaorder i , we compute overlapping metaorder volume during its execution window $[t_{s,i}, t_{e,i}]$. Let W_i^+ be the temporally prorated USD volume of native TWAPs in the same direction as the focal order, and let W_i^- be the corresponding volume of native TWAPs in the opposite direction. Let M_i denote the temporally prorated USD volume of other statistical metaorders overlapping the same window, excluding the focal order itself. We define

$$D_i^+ = \frac{W_i^+}{W_i^+ + W_i^- + M_i}, \quad D_i^- = \frac{W_i^-}{W_i^+ + W_i^- + M_i}. \quad (7)$$

Thus D_i^+ measures same-side visible TWAP dominance, while D_i^- measures opposite-side visible TWAP dominance. The aggregate dominance measure $D_i = D_i^+ + D_i^-$ pools these two components. Since same-side and opposite-side exposure have different economic content and, as shown below, opposite signs, the aggregate measure is not the appropriate object for testing the nonannouncer prediction.

A remaining concern is that the timing of the focal statistical metaorder may be related to visible TWAP activity. To separate TWAP flow that was already visible at the focal start from TWAPs that begin only later, we also construct already-visible versions of the dominance variables, $D_i^{+,vis}$ and $D_i^{-,vis}$. These variables are defined as in Eq. (7), but include only overlapping TWAP programs that had already started by the time the focal metaorder began, $t_{s,j}^{TWAP} \leq t_{s,i}$. Thus the TWAP program was observable to the market at the focal's arrival, while its subsequent child executions may still overlap the focal execution window.

We use the permanent impact $I_i^{perm}(\tau)$, defined in Eq. (4), as our outcome, evaluated both at completion ($\tau = 1$) and at the post-execution horizons $\tau \in \{1.5, 2, 3, 4\}$, each winsorized symmetrically at the 99% level. The completion value isolates the signed execution cost, while the post-execution horizons reveal whether the effect persists: a purely mechanical price-pressure effect should weaken after execution, whereas an adverse-selection effect should remain visible in permanent price displacement.

For each outcome $Y_i \in \{I_i^{perm}(\tau) : \tau \in \{1, 1.5, 2, 3, 4\}\}$ we estimate

$$Y_i = \alpha + \beta_+ D_i^+ + \beta_- D_i^- + \gamma' \mathbf{X}_i + \mu_{m(i)} + \lambda_{h(i)} + \delta_{d(i)} + u_i, \quad (8)$$

where $\mathbf{X}_i = (\log Q_i, \eta_i, \log T_i, N_i)$. The fixed effects are for market, start hour, and start day, and standard errors are clustered by start day. We also estimate the same specification replacing (D_i^+, D_i^-) with $(D_i^{+,vis}, D_i^{-,vis})$. The estimation sample applies the same restrictions used in the common-support analysis and contains 2,711,963 focal statistical metaorders across 199 markets and 239 start-day clusters.

Table 3 shows that same-side and opposite-side TWAP dominance have large effects of opposite sign. Using all overlapping TWAPs, the same-side coefficient is about +25 basis points per unit of dominance, whereas the opposite-side coefficient is about -30 basis points. Aggregating the two exposures would therefore obscure the relevant economics: same-side visible flow is associated with higher costs for latent traders in the same direction, whereas opposite-side visible flow works against the focal order direction.

The same-side effect is not a short-lived execution-window effect: the coefficient on D_i^+ is essentially unchanged from completion to the post-execution horizons, remaining between +23 and +25 basis points up to $\tau = 4$.

The already-visible specification provides the more conservative estimate. When dominance is computed only from TWAP programs already visible at the focal start, the same-side coefficient remains positive, highly significant, and stable across horizons. The estimates lie between +8.4 and +9.2 basis points per unit of dominance from completion through $\tau = 4$. Since dominance is a share, this corresponds to approximately 0.84–0.92 basis points for a 10 percentage point increase in already-visible same-side TWAP dominance. Economically, hidden orders executed in the direction of visible TWAP flow face higher permanent costs.

Outcome	$\hat{\beta}_+$	$\hat{\beta}_-$	$\hat{\beta}_+^{\text{vis}}$	$\hat{\beta}_-^{\text{vis}}$
$I_i^{\text{perm}}(1)$ (at completion)	+24.78*** (1.06)	-29.83*** (1.19)	+8.57*** (0.86)	-5.94*** (0.89)
$I_i^{\text{perm}}(1.5)$	+24.82*** (1.25)	-32.10*** (1.49)	+8.43*** (1.02)	-9.78*** (1.09)
$I_i^{\text{perm}}(2)$	+24.60*** (1.45)	-32.41*** (1.63)	+9.01*** (1.19)	-10.57*** (1.24)
$I_i^{\text{perm}}(3)$	+24.73*** (1.85)	-31.65*** (1.97)	+9.19*** (1.48)	-10.90*** (1.53)
$I_i^{\text{perm}}(4)$	+23.45*** (2.23)	-31.07*** (2.35)	+8.56*** (1.75)	-10.97*** (1.81)

Table 3: Side-decomposed regressions of permanent impact at and after completion on contemporaneous TWAP dominance. The + columns measure same-side TWAP dominance, while the - columns measure opposite-side TWAP dominance. Columns 2–3 use all overlapping TWAPs. Columns 4–5 restrict to TWAPs whose programs were already visible when the focal statistical metaorder started. Coefficients are in basis points for a unit increase in dominance, where dominance is a share between zero and one; standard errors, clustered by start day, are in parentheses. All specifications include controls ($\log Q_i, \eta_i, \log T_i, N_i$), market fixed effects, start-hour fixed effects, and start-day fixed effects. Significance: *** $p < 0.001$. The sample contains 2,711,963 observations and 239 start-day clusters.

The opposite-side coefficients have the opposite sign. In the already-visible specification, $\hat{\beta}_-^{\text{vis}}$ is negative at all horizons and grows in magnitude from about -6 basis points at completion to about -11 basis points by $\tau = 4$. Equivalently, a 10 percentage point increase in already-visible opposite-side TWAP dominance is associated with roughly 0.6–1.1 basis points lower permanent impact. This pattern is consistent with the opposite-side TWAP’s own price footprint benefiting the focal order mechanically; the direct test below confirms this reading.

A mechanical concern remains: the overlapping TWAP flow moves prices through its own, largely permanent, impact. We therefore add to Eq. (8) the square-root-law pressure of the overlapping flow on each side, $\sqrt{W_i^\pm/V_i^{\text{exec}}}$, together with the focal’s signed pre-start return. The latter changes nothing. The former matters: in the all-overlap specification the same-side coefficient falls from about +25 to +8 basis points, and the negative opposite-side effect is entirely absorbed by the price footprint of the opposite flow itself. The conservative already-visible coefficient, instead, moves only from +8.6 to +6.4 basis points at completion (standard error 2.9). What survives is therefore a composition effect. Conditional on the mechanical price pressure generated by overlapping flow, hidden metaorders executed while same-side demand is already visible still pay about 6 basis points more than hidden metaorders executed when that demand remains latent. This residual effect is consistent with the adverse-selection channel in Admati and Pfleiderer’s preannouncement mechanism.

The results therefore support the nonannouncer-side prediction of the Admati–Pfleiderer mechanism. The previous subsection shows that visible TWAP flow has a smaller permanent footprint than latent statistical metaorders. The present subsection shows the mirror effect: conditional on being latent, a statistical metaorder executed in the direction of already visible TWAP flow faces higher permanent costs, robustly to controlling for the price pressure of the visible flow itself. The same sorting channel that makes announced flow less costly is associated with higher costs for the hidden flow that remains on the same side.

This sorting is conditional: it operates within a market, in the direction of contemporaneous visible flow. A natural further question is whether it also surfaces as a cross-market *comparative*

static, since Admati and Pfleiderer’s sharpest prediction is that the cost saving from visible execution should be larger where adverse selection is more severe. We close by testing this prediction directly, and find that it does *not* hold against coarse market-wide measures of adverse selection: a null that, as we argue, pins down the level at which the mechanism operates rather than contradicting it.

For each market m we estimate the separable temporary-impact surfaces of Eq. (2) separately for the two channels and define the *announcer discount*

$$\Delta_m = \log_{10} \widehat{\mathcal{I}}_{\text{tmp}}^{\text{stat}}(\eta_m^*, F_m^*) - \log_{10} \widehat{\mathcal{I}}_{\text{tmp}}^{\text{TWAP}}(\eta_m^*, F_m^*), \quad (9)$$

at the market’s median common-support profile (η_m^*, F_m^*) ; Δ_m is the market-level analogue of the pooled discount $-\theta$ of Section 4.1. The discount is positive in the large majority of markets, so the announcer-cost result holds market by market.

We relate Δ_m to three market-level proxies for adverse-selection severity, all built from the trade tape: Kyle’s price-impact coefficient λ_m^{Kyle} , the R^2 of the same price-impact regression, and the lag-one autocorrelation of the sign of order flow [32, 23]. We take the order-flow autocorrelation as our preferred proxy because it is nearly orthogonal to volatility, whereas λ_m^{Kyle} and the price-impact R^2 co-move strongly with it. Writing s_m for a generic, standardized proxy, we run the cross-sectional regression

$$\Delta_m = b_0 + b_1 s_m + b_2 s_m^2 + \gamma' \mathbf{Z}_m + \varepsilon_m,$$

where the quadratic term allows the cost saving from visible execution to be non-monotone in adverse selection, and \mathbf{Z}_m controls for market size, volatility, and the concentration of taker volume, measured by a Herfindahl–Hirschman index of taker market shares. The prediction is $b_1 > 0$: the discount should widen where adverse selection is more severe. Instead, b_1 and b_2 are jointly insignificant for every proxy ($p > 0.28$), with point estimates if anything weakly negative. We also re-estimate the relation within market rather than across markets, on a market \times week panel of 1,973 cells spanning 122 markets and 34 weeks, with market and week fixed effects and standard errors clustered by market. This exploits how the discount moves over time within a given market, and it again leaves the relation flat: for the volatility-orthogonal proxy the linear coefficient is $\hat{b}_1 = -0.011$, with standard error 0.007, a joint p -value of 0.32, and a within- R^2 of 0.002. This within-market test has limited power, however: each market-week surface is estimated on only a few hundred orders, so the weekly discount is noisy and close to white noise from one week to the next, with a lag-one autocorrelation of just 0.075.

We read this null not as evidence against the mechanism but as a statement about the level at which it operates in our data. Admati and Pfleiderer’s comparative static is framed in terms of a market-wide intensity of adverse selection, which our coarse trade-tape proxies are meant to capture. The closely related nonannouncer mechanism, however, is conditional: it concerns the inference the market draws about the residual hidden flow once part of the liquidity demand becomes visible. Our side-decomposed regressions isolate exactly this conditional object, now resolved by direction, and there the prediction holds sharply: same-side visible dominance raises permanent hidden-flow costs by about 8–9 basis points. The Admati–Pfleiderer sorting therefore does appear in our data, but in this conditional, event-level form, rather than as a relationship between the announcer discount and a market-wide measure of adverse selection.

4.4 Liquidity Provision around Announced Orders

The final implication concerns the supply of liquidity around announced orders. Two channels in Admati and Pfleiderer point in the same direction. In the costly-entry model, liquidity suppliers can condition their participation on the realized announced demand and add liquidity around visible orders. In the informational model, even with no entry margin, liquidity suppliers already in the market who infer that the announced flow is relatively uninformed face less adverse

selection on that side and can quote more aggressively. Either way, displayed liquidity should adjust around visible execution.

Admati and Pfleiderer model liquidity supply in a stylized batch-auction setting rather than in a limit order book, so it does not speak directly to book-level quantities. Hyperliquid lets us go one step further: because the venue is a fully on-chain CLOB, we observe the liquidity-supply side directly, through displayed depth, order-book imbalance, and resting limit orders. We therefore adapt the liquidity-supply prediction to this CLOB setting and test whether the book changes during active native TWAP execution in a way consistent with a liquidity-supply response to visible order flow, without taking a stand on which channel drives it.

For the order-book analysis, we retain events with a duration of at least five minutes and notional size of at least 10,000 USD. For statistical metaorders, we additionally require at least ten child trades. We study book-level variables around order execution: relative spreads, displayed depth, order-book imbalance, and fixed-notional sweep costs.

All side-dependent book variables are oriented by order direction: for buy orders we evaluate liquidity on the ask side, and for sell orders on the bid side. After this orientation, positive imbalance, higher depth, and lower sweep costs all correspond to greater liquidity available to absorb the order flow. We measure these variables on each order-book snapshot and track them along event time around each order; in the figures event time is parametrized by normalized order time $\tau = t/T_i$, while in the panel regressions below it is the relative clock minute m from the order start. For a given snapshot, let $B^{(k)}$ and $A^{(k)}$ denote displayed bid and ask size accumulated over all book levels whose prices are no farther than k quoted spreads from the midprice. This gives a local measure of displayed liquidity near the touch, while scaling the window by the spread makes it adaptive to differences in tightness across assets and market conditions. We define the oriented imbalance as

$$\text{Imb}^{(k)} = s \frac{B^{(k)} - A^{(k)}}{B^{(k)} + A^{(k)}}, \quad s = \begin{cases} -1, & \text{buy order,} \\ 1, & \text{sell order.} \end{cases}$$

Thus positive values always mean that displayed depth is tilted toward the absorbing side. We set $k = 5$, so the band spans five times the quoted spread. Depth is the corresponding dollar depth on that side, accumulated within the same band. Relative spread is $(a^1 - b^1)/\text{mid}$, reported in basis points. Fixed-notional sweep cost is the additional cost, relative to execution at the midprice, of immediately executing a fixed USD notional on the absorbing side of the book; all sweep-cost outcomes are reported in basis points.

Intuitively, under the sunshine-trading interpretation, the predicted signs are outcome-specific. A broad liquidity-supply response should appear away from the touch: imbalance should rise, depth should rise, and fixed-notional sweep costs should fall. These three are the signs of a book that becomes more able to absorb the announced flow while the program is active. The quoted spread is the ambiguous one: liquidity providers may widen the inside quote to protect themselves during a predictable execution window even as they supply more depth deeper in the book, so a narrowing spread is not a necessary implication.

Figure 7 compares the descriptive book dynamics around visible native TWAPs with those around latent statistical metaorders, separately for short, medium, and long metaorder durations. The most striking TWAP pattern is in the first column, the oriented imbalance measured within five times the quoted spread of the mid, which rises sharply at the start of the execution window. Under this convention, native TWAPs show a marked increase in imbalance during the active interval, clearest at short and medium durations, where it jumps at $\tau = 0$ and persists until completion. This is consistent with the book tilting toward the side able to absorb the announced flow. Statistical metaorders also display positive imbalance, but the increase is more gradual and tends to peak around completion rather than at the start. This is consistent with the fact that they are not publicly announced at $\tau = 0$, but may become progressively inferable during execution from same-address, same-direction trading. The duration split supports this

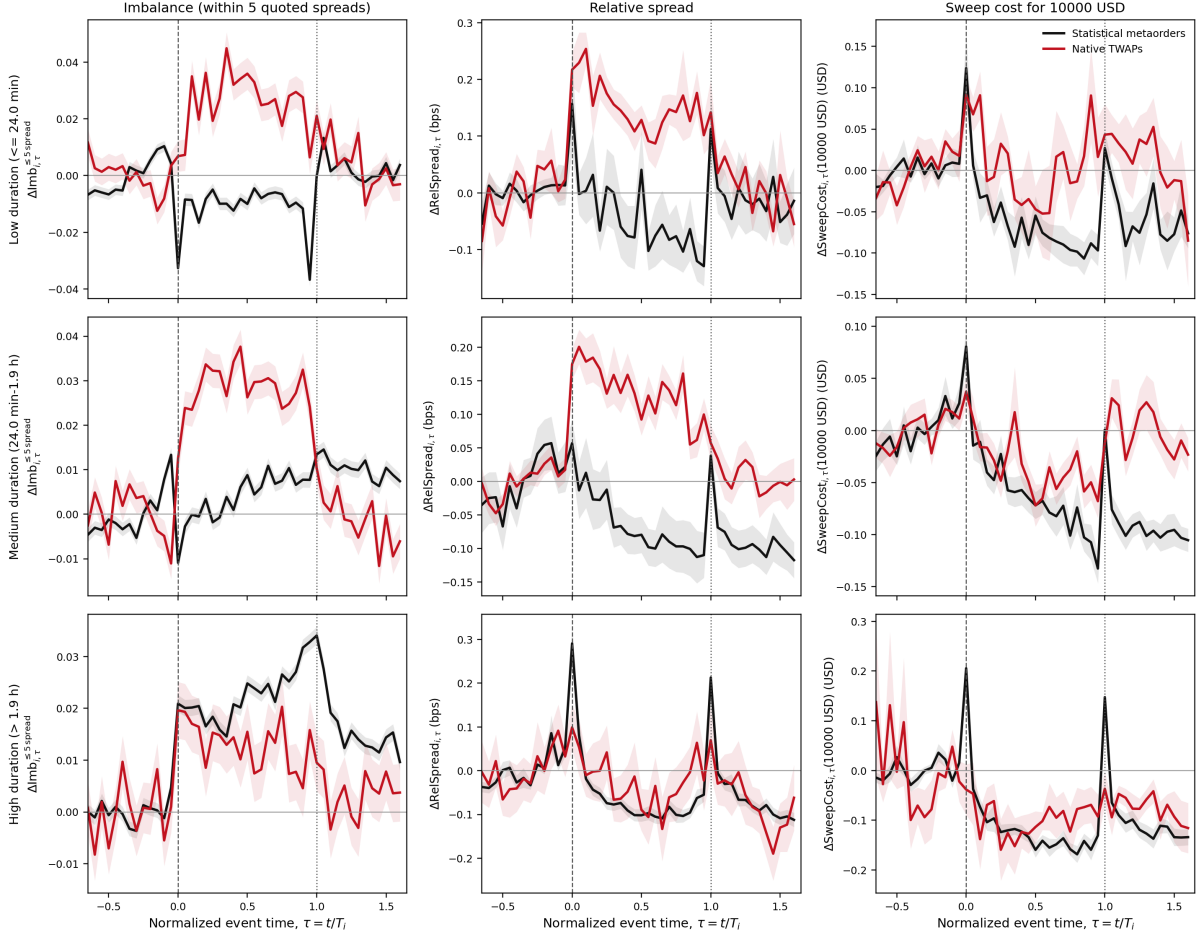


Figure 7: Order-book liquidity measures over normalized order time for native TWAPs and statistically reconstructed metaorders, split by metaorder clock-time duration. The columns report oriented imbalance within five times the quoted spread of the midprice, relative spread in basis points, and the cost in basis points of sweeping 10,000 USD; the rows correspond to short ($T_i < 24$ min), medium (24 min–1.9 h), and long ($T_i > 1.9$ h) durations. The horizontal axis is $\tau = t/T_i$, with $\tau = 0$ denoting order start and $\tau = 1$ denoting completion, and the displayed window runs from -0.65 to 1.65 order durations. Each series reports the change relative to its event-level pre-window mean. Variables are oriented to the side of the book opposite the order direction. Black lines denote statistically reconstructed metaorders and red lines denote native TWAPs; shaded bands denote ± 1 standard error.

interpretation: for longer statistical metaorders, imbalance rises more persistently over the execution window, suggesting that market makers learn that a given address is carrying out a directional program even without an explicit TWAP announcement. For shorter statistical metaorders, the book dynamics also reflect the U-shaped execution schedule documented above. The more aggressive child trades near the beginning and the end of the program put stronger immediate pressure on the book, which can depress oriented imbalance and raise both relative spreads and fixed-notional sweep costs around the execution edges.

The spread and sweep-cost panels reveal a distinction between quoted liquidity at the touch and executable liquidity deeper in the book. Native TWAPs exhibit a positive relative-spread response after the start of execution, so the inside quote becomes more expensive rather than narrower. At the same time, the cost of sweeping a fixed notional falls during the active TWAP interval, indicating that walking the book becomes cheaper even though the best quotes widen. This combination is not necessarily paradoxical. Once a large order is announced, liquidity

suppliers may be willing to absorb the predictable order flow only at prices that compensate them for the expected inventory risk. In a limit-order book, this can appear as a wider inside spread together with more depth away from the best quote on the absorbing side. The book therefore need not become cheaper at the very touch in order to become more able to absorb the announced flow. This reading is consistent with concurrent evidence that liquidity provision on Hyperliquid is dominated by high-frequency market-making strategies competing aggressively for queue priority through large volumes of post-only orders [28]. Both patterns are visible across the duration buckets and are sharpest at short and medium durations.

Since the figure is descriptive, we complement it with an event-time placebo regression that isolates whether liquidity changes differentially during the active TWAP window, net of event baselines and common event-time patterns.

We implement the TWAP liquidity-response test with an event-time placebo design. For event i and relative minute m , we estimate

$$y_{i,m} = \alpha_i + \lambda_m + \beta \mathbb{1}\{\text{TWAP}_i\} \mathbb{1}\{0 \leq m \leq T_i\} + u_{i,m}. \quad (10)$$

Here $y_{i,m}$ is one of the book-level liquidity measures defined above (oriented imbalance, displayed depth, relative spread, or fixed-notional sweep cost), α_i are event fixed effects, and λ_m are relative-minute fixed effects. The treatment indicator equals one only for observations belonging to real native TWAP events during their active execution window. Placebo starts drawn from the same order-book panel provide the comparison group. The coefficient β therefore measures whether liquidity changes differentially during the active TWAP window, relative to event-specific baselines and common event-time patterns. Standard errors are clustered by event.

Table 4 turns the descriptive figure into event-time placebo regressions for native TWAPs, pooled across durations. The regression uses the same within-five-quoted-spread imbalance and depth measures as Figure 7. During the active TWAP window, relative spreads are about 0.28 basis points higher than in the placebo comparison, so the inside quote does not improve. Away from the touch, however, the signs are all favorable: imbalance increases by 0.022, depth rises by about 4,200 USD, and the 10,000 USD sweep cost falls by 0.025 basis points.

We probe two further questions by augmenting Eq. (10). Define $A_{i,m} = \mathbb{1}\{\text{TWAP}_i\} \mathbb{1}\{0 \leq m \leq T_i\}$ for the active-window indicator. First, to check that the active-window estimates are not an artifact of a differential pre-trend, we add a pre-window lead $L_{i,m} = \mathbb{1}\{\text{TWAP}_i\} \mathbb{1}\{m < 0\}$ and estimate

$$y_{i,m} = \alpha_i + \lambda_m + \beta A_{i,m} + \delta L_{i,m} + u_{i,m}; \quad (11)$$

under a clean event interpretation the change occurs at the announcement, so $\hat{\delta}$ should be close to zero. Second, to ask whether the response scales with the size of the announced program, we interact the active window with the log notional measured relative to its sample median, $q_i = \log(Q_i/Q_{\text{med}})$, where Q_{med} is the median announced notional (about 49,000 USD), and estimate

$$y_{i,m} = \alpha_i + \lambda_m + \beta A_{i,m} + \zeta A_{i,m} q_i + u_{i,m}; \quad (12)$$

a positive $\hat{\zeta}$ on the displayed-liquidity outcomes is the sharpest version of the costly-entry channel, in which a larger visible order summons a larger book response. Table 4 reports $\hat{\delta}$ and $\hat{\zeta}$ alongside the baseline $\hat{\beta}$.

The pre-window lead confirms that the favorable book responses are not pre-trends. For imbalance, depth, and the sweep cost the lead coefficient is economically negligible and, where significant, of the opposite sign to the active-window effect: the imbalance lead is about three percent of the active-window estimate, and the depth and sweep-cost leads are essentially zero. The exception is the relative spread, whose lead (+0.21 bps) is of the same order as its active-window coefficient (+0.28 bps): much of the spread widening is already present before the program becomes active, although it continues to increase during the active TWAP window.

Book outcome	Active window $\hat{\beta}$	Pre-window lead $\hat{\delta}$	Size interaction $\hat{\zeta}$
Relative spread (bps)	0.277*** (0.029)	0.210*** (0.019)	-0.024 (0.013)
Imbalance, 5 \times spread	0.0219*** (0.0012)	-0.0007** (0.0003)	0.0028*** (0.0008)
Depth, 5 \times spread (USD)	4182* (1801)	-222 (432)	3499** (1264)
Sweep cost, 10,000 USD (bps)	-0.0250*** (0.0073)	0.0016 (0.0027)	0.0288*** (0.0038)

Table 4: Event-time liquidity response during active native TWAP execution, pooled across durations. Each cell reports a coefficient with its event-clustered standard error in parentheses. $\hat{\beta}$ is the active-window effect from Eq. (10); $\hat{\delta}$ is the pre-window lead from Eq. (11), with a value near zero indicating no differential pre-trend; $\hat{\zeta}$ is the size interaction from Eq. (12). Positive imbalance and depth, and negative sweep-cost coefficients, indicate a book more able to absorb the announced flow. Imbalance and depth are accumulated over all book levels within five times the quoted spread of the midprice. The sample has about 9.4 million event-minute observations across 56,692 events. Significance: * $p < 0.05$, ** $p < 0.01$, *** $p < 0.001$.

A comparison with statistical metaorders helps clarify the spread lead. Latent metaorders begin execution in book states with relative spreads about 0.16 bps above matched placebo windows, close to the 0.21 bps elevation of native TWAPs, but they show only a much smaller widening of the inside quote at the start itself, about 0.05 bps, against 0.17 bps for TWAPs. The level of the spread before execution is thus a property of the market states in which sizable directional programs are initiated, shared by visible and latent execution, while only the additional, announcement-coincident widening of the touch is specific to native TWAPs. We accordingly read the spread lead as selection into wider-spread states rather than as a response to TWAP visibility.

The size interaction shows that the displayed-liquidity response scales with the announced size. The coefficient is positive and strongly significant for imbalance. A one-log-unit increase in announced notional, corresponding to roughly a 2.7 \times larger program, raises the imbalance response by $\hat{\zeta} = +0.0028$, about one eighth of the baseline effect. The coefficient is also positive and significant for depth: larger visible programs are met with a larger tilt of the book toward the absorbing side and with more displayed depth, exactly the comparative static implied by suppliers conditioning on the realized announced demand. The executable-cost improvement, by contrast, does not scale: the sweep-cost interaction is positive, so the cost reduction is, if anything, smaller for larger orders.

Overall, the order-book evidence points to a liquidity-supply response around active native TWAP execution. During the active window, the book becomes more tilted toward the absorbing side, displayed depth increases, and fixed-notional sweep costs fall, while quoted spreads widen. This pattern is consistent with the book preparing to absorb the announced order flow at the prices at which liquidity suppliers are willing to bear the associated inventory risk. In this sense, visible TWAPs are associated with a book that becomes more able to accommodate the announced execution, rather than simply with more aggressive inside quotes. These responses are not explained by favorable pre-trends and, for displayed-liquidity measures, they scale with the size of the announced program.

5 Limitations

Several limitations qualify the interpretation of the evidence. First, because the main analysis is market-order based, it can also classify very active liquidity providers as metaorder executors when they repeatedly cross the spread in the same direction. A filled-limit-order diagnostic illustrates the issue. In the population of reconstructed metaorders with at least ten child orders, 46.2% have at least one same-address maker fill during the execution window and 40.3% have a same-direction maker fill. This passive volume, however, is highly concentrated: the top 40 addresses by passive maker-fill volume account for about 68% of all passive same-address maker-fill USD and about 65% of same-direction passive USD. These addresses also display both same- and opposite-direction maker fills, consistent with market-maker-like activity rather than a diffuse pattern of metaorders being executed passively. After excluding these top-40 passive-volume addresses, the same-direction maker-fill rate falls to about 31%. We therefore keep the market-orders-only definition as the main object and treat the filled-limit-order evidence as a contamination and classification caveat, rather than as a correction to metaorder size or participation.

Second, the contrast between native TWAPs and statistical metaorders is observational. Traders choose whether to use the protocol-native TWAP tool, and this choice is strongly tied to trader identity. In an out-of-sample horse race, a pair-only model has AUC 0.674, adding pre-start book state raises it only to 0.685, while a taker-identity prior reaches AUC 0.998; the between-taker share of variation in the TWAP/statistical choice is about 0.93. In the full sample, 86.6% of orders are generated by taker addresses that exclusively use one of the two mechanisms. A caveat is that addresses need not map one-to-one to traders. Hyperliquid natively supports sub-accounts, which share the master account’s volume-based fee tier and are therefore the natural way to separate strategies across wallets; sub-accounts, however, are publicly linkable to their master account on chain. Aggregating native sub-accounts to their master accounts (we map the addresses accounting for 99.7% of sample volume) leaves the picture essentially unchanged: the share of orders from single-mechanism units moves from 86.6% to 85.4%, and only 39 entities, accounting for 0.24% of volume, consist of pure-TWAP and pure-statistical wallets combined under one master. Splitting flow across independent, unlinkable wallets is instead pecuniarily costly, since fee tiers are computed per account on rolling 14-day volume, so fragmenting volume permanently worsens each wallet’s fee schedule. Mechanism segregation is thus a property of entities, not an artifact of wallet splitting. These numbers show that the comparison is between execution regimes populated by different trader types, not a randomized comparison of the same trader choosing two mechanisms under otherwise identical conditions.

Third, “hidden” statistical metaorders are not hidden in the same sense as anonymous institutional metaorders in traditional markets. Every trade on Hyperliquid reports an address, so same-address, same-direction trading can be statistically inferred while it is unfolding. The distinction we exploit is therefore between explicit protocol-level preannouncement of the metaorder and gradual statistical inferability from address-level flow. This matters for the order-book interpretation: the gradual increase in oriented book imbalance around statistical metaorders may reflect market participants learning from repeated address-level trades, whereas native TWAPs reveal the execution program directly from inception. The statistical-metaorder benchmark is therefore a latent but partially learnable execution regime, not a perfectly anonymous hidden-flow benchmark.

Fourth, market-state predictability is limited. In a discrete-time arrival exercise on five-minute bins, dynamic book and flow state improves PR-AUC for TWAP starts only from 0.0033 under a pair-hour climatology to 0.0053, whereas the improvement for statistical-metaorder starts is larger, from 0.094 to 0.142. This suggests that market state is more useful for identifying regimes with high statistical-metaorder hazard than for forecasting the precise start of a native TWAP. Conditional on an order arriving, trader identity dominates book state. The paper

should therefore not be read as showing that the book strongly predicts individual TWAP arrivals.

Finally, Hyperliquid is an environment with visible addresses and a protocol-native, low-friction TWAP mechanism. These features are central to the identification strategy, but they also mean that the mapping to anonymous traditional markets or to venues without a native TWAP facility should be made with care.

6 Conclusion

This paper studies market impact on Hyperliquid, a setting in which both execution paths and execution mechanisms are unusually transparent. Protocol-native TWAP orders are publicly visible while active and therefore constitute a protocol-level form of sunshine trading, whereas statistically reconstructed metaorders are inferred only ex post. This contrast lets us compare not two execution algorithms but two execution regimes that differ in ex-ante observability, along the dimensions of temporary impact, impact trajectories, execution schedules, post-trade relaxation, and the surrounding order book.

We first establish that native TWAPs have systematically lower temporary impact than statistical metaorders over a broad range of traded fractions, and that the two classes differ sharply in dynamics: TWAP trajectories and schedules are smooth and close to the square-root benchmark associated with uniform execution, whereas statistical metaorders display U-shaped schedules, stronger trajectory curvature, a local peak around completion, and a larger permanent price displacement. These patterns are consistent with a transient-impact interpretation of strategic execution.

We then read the comparison through the four mechanisms of Admati and Pfleiderer. Visible TWAPs face lower costs as announcers, and their flow is less informationally adverse, leaving a smaller permanent price footprint. The mirror cost falls on nonannouncers, since hidden flow executed in the same direction as already-visible TWAP activity is priced as more adversely selected. The order book also responds to visible execution. Concretely, during the active TWAP window the book becomes asymmetric: more displayed size accumulates on the side that has to absorb the announced flow than on the opposite side, so that our oriented imbalance measure rises. Total displayed depth near the touch increases as well, and as a result the cost of sweeping a fixed notional falls. The inside spread, by contrast, widens rather than narrows: liquidity suppliers do not quote more aggressively at the best bid and ask, but instead rest additional size slightly behind the touch, at the prices at which they are willing to fill the predictable order and be compensated for the inventory risk they take on. All of these displayed-liquidity responses scale with the announced size.

Overall, the evidence is consistent with a sunshine-trading interpretation: on Hyperliquid, publicly visible TWAP flow appears less informed on average, and its visibility elicits liquidity provision rather than triggering predatory front-running. More broadly, Hyperliquid provides a rare empirical setting in which the costs and benefits of pre-trade transparency can be studied directly rather than inferred indirectly.

References

- [1] A. S. Kyle, “Continuous auctions and insider trading,” *Econometrica*, pp. 1315–1335, 1985.
- [2] R. Almgren, C. Thum, E. Hauptmann, and H. Li, “Direct estimation of equity market impact,” *Risk*, vol. 18, no. 7, pp. 58–62, 2005.
- [3] B. Tóth, Y. Lemperiere, C. Deremble, J. De Lataillade, J. Kockelkoren, and J.-P. Bouchaud, “Anomalous price impact and the critical nature of liquidity in financial markets,” *Physical Review X*, vol. 1, no. 2, p. 021006, 2011.
- [4] J. Donier and J. Bonart, “A million metaorder analysis of market impact on the Bitcoin,” *Market Microstructure and Liquidity*, vol. 1, no. 02, p. 1550008, 2015.
- [5] B. Tóth, Z. Eisler, and J.-P. Bouchaud, “The square-root impact law also holds for option markets,” *Wilmott*, vol. 2016, no. 85, pp. 70–73, 2016.
- [6] E. Zarinelli, M. Treccani, J. D. Farmer, and F. Lillo, “Beyond the square root: Evidence for logarithmic dependence of market impact on size and participation rate,” *Market Microstructure and Liquidity*, vol. 1, no. 2, p. 1550004, 2015.
- [7] J. Donier, J. Bonart, I. Mastromatteo, and J.-P. Bouchaud, “A fully consistent, minimal model for non-linear market impact,” *Quantitative Finance*, vol. 15, no. 7, pp. 1109–1121, 2015.
- [8] M. Benzaquen and J.-P. Bouchaud, “Market impact with multi-timescale liquidity,” *Quantitative Finance*, vol. 18, no. 11, pp. 1781–1790, 2018.
- [9] F. Bucci, M. Benzaquen, F. Lillo, and J.-P. Bouchaud, “Crossover from linear to square-root market impact,” *Physical Review Letters*, vol. 122, no. 10, p. 108302, 2019.
- [10] E. Moro, J. Vicente, L. G. Moyano, A. Gerig, J. D. Farmer, G. Vaglica, F. Lillo, and R. N. Mantegna, “Market impact and trading profile of hidden orders in stock markets,” *Physical Review E*, vol. 80, no. 6, p. 066102, 2009.
- [11] X. Brokmann, E. Serie, J. Kockelkoren, and J.-P. Bouchaud, “Slow decay of impact in equity markets,” 2014.
- [12] E. Bacry, A. Iuga, M. Lasnier, and C.-A. Lehalle, “Market impacts and the life cycle of investors orders,” Nov. 2014.
- [13] H. Waelbroeck and C. Gomes, “Is market impact a measure of the information value of trades? market response to liquidity vs. informed trades,” 2013. Working paper / SSRN.
- [14] A. R. Admati and P. Pfleiderer, “Sunshine trading and financial market equilibrium,” *The Review of Financial Studies*, vol. 4, no. 3, pp. 443–481, 1991.
- [15] T. Schöneborn and A. Schied, “Liquidation in the face of adversity: Stealth vs. sunshine trading.” EFA 2008 Athens Meetings Paper, Mar. 2009. Date written: March 18, 2009. Available at SSRN.
- [16] J. A. Skjeltorp, E. Sojli, and W. W. Tham, “Sunshine trading: Flashes of trading intent at the Nasdaq,” Tech. Rep. Discussion Paper 12-141/IV, Tinbergen Institute, 2012.
- [17] H. Bessembinder, A. Carrion, L. A. Tuttle, and K. Venkataraman, “Liquidity, resiliency and market quality around predictable trades: Theory and evidence,” *Journal of Financial Economics*, vol. 121, no. 1, pp. 142–166, 2016.

- [18] P. Daian, S. Goldfeder, T. Kell, Y. Li, X. Zhao, I. Bentov, L. Breidenbach, and A. Juels, “Flash boys 2.0: Frontrunning, transaction reordering, and consensus instability in decentralized exchanges,” in *2020 IEEE Symposium on Security and Privacy*, pp. 910–927, IEEE, 2020.
- [19] L. Zhou, K. Qin, C. F. Torres, D. V. Le, and A. Gervais, “High-frequency trading on decentralized on-chain exchanges,” in *2021 IEEE Symposium on Security and Privacy*, pp. 428–445, IEEE, 2021.
- [20] K. Qin, L. Zhou, and A. Gervais, “Quantifying blockchain extractable value: How dark is the forest?,” in *2022 IEEE Symposium on Security and Privacy*, pp. 198–214, IEEE, 2022.
- [21] Hyperliquid Foundation, “Hyperliquid Documentation.” <https://hyperliquid.gitbook.io/hyperliquid-docs>, 2026. Accessed: 2026-06-01.
- [22] J.-P. Bouchaud, J. Bonart, J. Donier, and M. Gould, *Trades, Quotes and Prices: Financial Markets Under the Microscope*. Cambridge University Press, 2018.
- [23] F. Lillo and J. D. Farmer, “The long memory of the efficient market,” *Studies in Nonlinear Dynamics & Econometrics*, vol. 8, no. 3, 2004.
- [24] B. Tóth, I. Palit, F. Lillo, and J. D. Farmer, “Why is equity order flow so persistent?,” *Journal of Economic Dynamics and Control*, vol. 51, pp. 218–239, 2015.
- [25] M. Yin, D. Malkhi, M. K. Reiter, G. G. Gueta, and I. Abraham, “HotStuff: BFT consensus with linearity and responsiveness,” in *Proceedings of the 2019 ACM Symposium on Principles of Distributed Computing (PODC ’19)*, ACM, 2019.
- [26] Hydromancer, “Reservoir: Hyperliquid Historical Data.” <https://docs.hydromancer.xyz/reservoir>, 2026. Accessed: 2026-05-27.
- [27] J. Albers, M. Cucuringu, S. Howison, and A. Y. Shestopaloff, “An open book: Level 4 order book data from the Hyperliquid exchange,” Mar. 2026. SSRN Working Paper.
- [28] J. Albers, M. Cucuringu, S. Howison, and A. Y. Shestopaloff, “The “Neutrinos” of the order book: Pervasive, weakly interacting order flow and its consequences,” Feb. 2026. SSRN Working Paper.
- [29] M. Parkinson, “The extreme value method for estimating the variance of the rate of return,” *The Journal of Business*, vol. 53, no. 1, pp. 61–65, 1980.
- [30] J. Gatheral, “No-dynamic-arbitrage and market impact,” *Quantitative Finance*, vol. 10, no. 7, pp. 749–759, 2010.
- [31] J. Gatheral, A. Schied, and A. Slynko, “Transient linear price impact and Fredholm integral equations,” *Mathematical Finance*, vol. 22, no. 3, pp. 445–474, 2012.
- [32] J. Hasbrouck, “Measuring the information content of stock trades,” *The Journal of Finance*, vol. 46, no. 1, pp. 179–207, 1991.
- [33] J.-P. Bouchaud, Y. Gefen, M. Potters, and M. Wyart, “Fluctuations and response in financial markets: the subtle nature of “random” price changes,” *Quantitative Finance*, vol. 4, no. 2, pp. 176–190, 2003.

A Appendix: A Transient-Impact Benchmark

To interpret the empirical patterns, we consider a simple transient-impact benchmark based on a propagator model [33, 23, 30]. The model is written in model time $v \in [0, F]$, where F denotes the execution horizon:

$$s(v) = s(0) + \int_0^v q(u) G(v - u) du + W_v,$$

where $q(u)$ is the signed execution rate, $G(\cdot)$ is the transient-impact kernel, and W_v captures exogenous price fluctuations. The execution rate is the infinitesimal counterpart of the cumulative schedule: if $C(v)$ denotes the fraction of an order of size $Q(F)$ executed by time v , then

$$C(v) = \frac{1}{Q(F)} \int_0^v q(u) du, \quad C(F) = 1.$$

Thus different execution schedules C correspond to different trading rates q , and therefore to different impact trajectories.

We use a linear propagator with a power-law decay kernel,

$$G(t) \propto t^{-\rho}, \quad \rho = \frac{1}{2}.$$

Once the kernel is fixed, the deterministic shape of the impact trajectory is driven by the execution schedule. In particular, under a constant-rate schedule $q(u) = q_0$,

$$\int_0^v q_0(v - u)^{-1/2} du \propto \sqrt{v}.$$

Thus a constant-rate schedule naturally produces a square-root-like impact trajectory, providing a simple benchmark for native TWAP execution.

The same framework also explains why non-linear schedules can generate the double-inflection trajectories observed for statistical metaorders. We compute optimal schedules from a mean-variance-style objective that trades off expected transient-impact cost against a quadratic penalty on remaining inventory,

$$\min_q \mathcal{C}(q) + \lambda \mathcal{R}(q), \quad \int_0^F q(u) du = Q(F),$$

where $\mathcal{C}(q)$ is the expected impact-cost component, $\mathcal{R}(q)$ is the inventory-risk component, and $\lambda \geq 0$ indexes risk aversion. When $\lambda = 0$, the risk-neutral optimum in this transient-impact benchmark is U-shaped, with faster trading near the beginning and the end of the execution interval. Increasing λ shifts the schedule toward the beginning of the interval, because the trader puts more weight on reducing unfinished exposure. The benchmark therefore provides a parsimonious mechanism linking the execution schedules in Figure 4 to the impact trajectories in Figure 3.

Figure 8 illustrates this mechanism for four values of λ . The blue curves report the during-execution impact paths generated by optimal schedules with different horizons F , and the black dots mark completion. The red curve is the corresponding temporary impact at completion, $\mathcal{I}_{\text{tmp}}(F)$, interpolated across horizons. In the top row the participation rate is fixed, so $Q(F) = \eta F$ and temporary impact rises with F . In the bottom row total size is fixed, so $Q(F) = Q_0$ and longer execution lowers participation. Moving from left to right, higher risk aversion front-loads execution and makes impact peak earlier, producing non-concave during-execution shapes similar to those observed for statistical metaorders. The exercise is not intended as a structural calibration of the model, but as a qualitative benchmark showing that the empirical shapes are consistent with transient-impact dynamics.

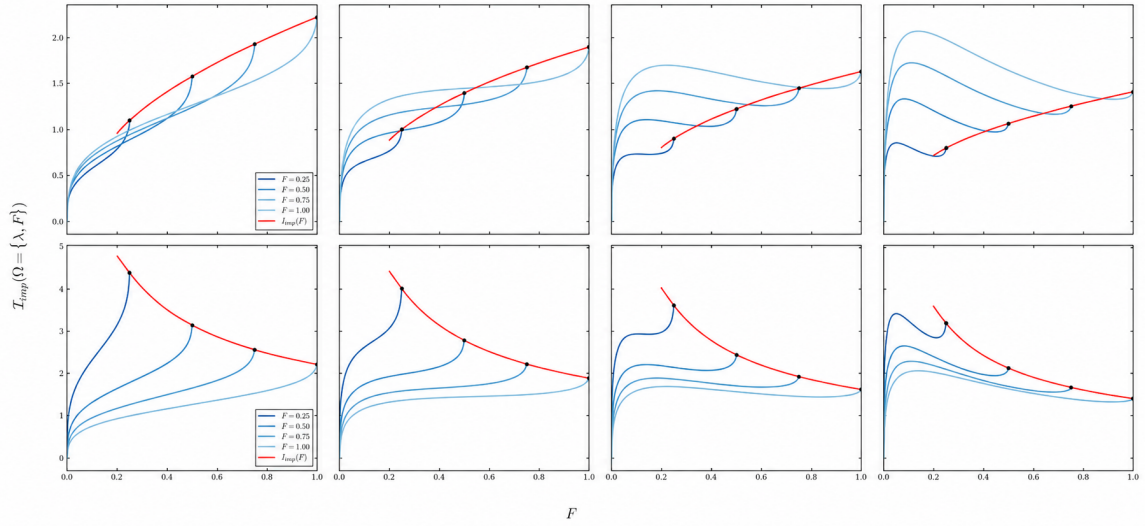


Figure 8: Impact trajectories generated by optimal schedules in the propagator model. Each column corresponds to a different level of risk aversion λ . Blue curves show the signed impact trajectory during execution for different horizons F ; black dots mark completion. The red curve reports the corresponding temporary impact at completion, $\mathcal{I}_{\text{tmp}}(F)$. The top row fixes the participation rate, so that $Q(F) = \eta F$, and the bottom row fixes total size, so that $Q(F) = Q_0$. As λ increases, optimal schedules become more front-loaded.